

공학석사학위논문

Formulation of P-M Interaction Diagram
by Applying Uniformly Distributed Reinforcement and
Determination of RC Pylon Sections for Target Reliability

등분포 철근 정식화를 적용한 PM 상관도 작성 및
목표신뢰도를 만족하는 RC 주탑 단면 결정

2016 년 8 월

서울대학교 대학원

건설환경공학부

최 윤 승

ABSTRACT

This paper suggests a method to determine the optimum cross sections of RC pylons that satisfy the target reliability level. P-M interaction diagram is formulated based on uniformly distributed reinforced concrete to generalize the strength of RC column sections. Reliability analysis is conducted by HL-RF algorithm with gradient projection method. An optimum section that satisfies the target reliability level is determined for one of transverse and longitudinal direction or both of them. Object function is selected for reliability index requirement and the equation is solved by Newton-Raphson method with reinforcement equation or regularization function. The validity of method is demonstrated for two pylon section examples, Inchoen Bridge and Ulsan Bridge. When the reinforcement equation and regularization function are used for finding optimum sections, respectively, it is verified that the results are in agreement with each other under same reinforcement ratio condition. The feasibility of optimum section with general rebar is checked by placing the equivalent rebar in the cross section

KEY WORDS:

Optimum pylon section, P-M interaction diagram, Reliability analysis, Target reliability index, Uniformly distributed reinforcement, Regularization function.

Student Number: 2014-20560

Table of Contents

1. Introduction	1
2. Reliability Assessment of RC pylon section.	2
2.1 Basic Theory of Reliability Assessment	2
2.2 AFOSM with gradient projection	6
2.3 Rackwitz-Fiessler transformation	10
3. Uniformly Distributed Reinforcement	12
3.1 Definition of Uniformly Distributed Reinforcement	12
3.2 PMID of Uniformly Distributed Reinforced Concrete Column	13
3.3 Reliability Assessment of RC pylon cross section	17
3.4 Comparison of Reliability Index for discrete and uniformly distributed reinforced RC column	25
4. Optimization of pylon section for Target Reliability.	28
4.1 General method	28
4.2 Determination of RC pylon Sections for Uniaxial Target reliability ..	30
4.3 Determination of RC pylon Sections for Biaxial Target reliability ..	33
5. Application and Verification	36
5.1 Incheon Bridge	37
5.1.1 Result of reliability analysis	40
5.1.2 Determination of pylon section for uniaxial target reliability	41
5.1.3 Determination of pylon section for biaxial target reliability	45
5.2 Ulsan Bridge	51
5.2.1 Result of reliability analysis	54
5.2.2 Determination of pylon section for uniaxial target reliability	56
5.2.3 Determination of pylon section for biaxial target reliability	59

6. Summary and Conclusion 64
Reference 66

List of Figures

Fig. 2.1 Probabilistic concept of reliability index	4
Fig. 2.2 Definition of limit state in random variable space.....	5
Fig. 2.3 Reliability index in standard normal space (Hasofer-Lind)	6
Fig. 3.1 Equivalent uniformly distributed reinforced concrete.....	13
Fig. 3.2 Typical cross section of an RC column and PMID	14
Fig. 3.3 Limit state function of RC columns	17
Fig. 3.4 PMID approximated by cubic spline.....	18
Fig. 3.5 Cross section of example RC column.....	25
Fig. 3.6 Nominal and limit PMIDs and MPFPs of example section	27
Fig. 5.1 Pylon and cross section of Incheon Bridge.....	37
Fig. 5.2 Nominal and limit PMIDs and MPFPs of Incheon Bridge in transverse direction.....	40
Fig. 5.3 Dimension scale of geometric parameters for uniaxial target reliability under given reinforcement ratio	42
Fig. 5.4 Dimension scale of geometric parameters for uniaxial target reliability under given regularization function	42
Fig. 5.5 Comparison of results for condition of reinforcement ratio and regularization function.....	43
Fig. 5.6 Optimum section for uniaxial target reliability of 4% reinforcement ratio with general rebar.....	44
Fig. 5.7 Nominal and limit PMIDs and MPFPs for 4% reinforcement cross section	44
Fig. 5.8 Dimension scale of geometric parameters for biaxial target reliability Under given reinforcement ratio.....	46

Fig. 5.9 Dimension scale of geometric parameters for biaxial target reliability under given regularization function.....	46
Fig. 5.10 Comparison of results for condition of reinforcement ratio and regularization function	47
Fig. 5.11 Optimum section for biaxial target reliability of 4% reinforcement ratio with general rebar.....	48
Fig. 5.12 Nominal and limit PMIDs and MPFPs for 4% reinforcement cross section in transverse direction	49
Fig. 5.13 Nominal and limit PMIDs and MPFPs for 4% reinforcement cross section in longitudinal direction.....	50
Fig. 5.14 Pylon and cross section of Ulsan Bridge.....	51
Fig. 5.15 Nominal and limit PMIDs and MPFPs of Ulsan Bridge in transverse direction	54
Fig. 5.16 Nominal and limit PMIDs and MPFPs of Ulsan Bridge in longitudinal direction.....	55
Fig. 5.17 Dimension scale of geometric parameters for uniaxial target reliability under given reinforcement ratio.....	56
Fig. 5.18 Dimension scale of geometric parameters for uniaxial target reliability under given regularization function.....	57
Fig. 5.19 Comparison of results for condition of reinforcement ratio and regularization function.....	57
Fig. 5.20 Optimum section for uniaxial target reliability of 2% reinforcement ratio with general rebar.....	58
Fig. 5.21 Nominal and limit PMIDs and MPFPs for 2% reinforcement cross section	58
Fig. 5.22 Dimension scale of geometric parameters for biaxial target reliability under given reinforcement ratio	60

Fig. 5.23 Dimension scale of geometric parameters for biaxial target reliability under given regularization function	60
Fig. 5.24 Comparison of results for condition of reinforcement ratio and regularization function.....	61
Fig. 5.25 Optimum section for biaxial target reliability of 2% reinforcement ratio with general rebar	61
Fig. 5.26 Nominal and limit PMIDs and MPFPs for 2% reinforcement cross section in transverse direction	62
Fig. 5.27 Nominal and limit PMIDs and MPFPs for 2% reinforcement cross section in longitudinal direction.....	63

List of Tables

Table 3.1 Statistical properties of random variables in example section.....	26
Table 3.2 External load effect of example section.....	26
Table 3.3 Reliability index and normalized MPFP of example section.....	27
Table 5.1 Statistical properties of random variables for cross section of Incheon Bridge pylon	38
Table 5.2 Load effect of cross section of Incheon Bridge pylon.....	39
Table 5.3 Composition of wind load of Incheon Bridge.....	39
Table 5.4 Reliability index and normalized MPFP of Incheon Bridge in transverse direction.....	40
Table 5.5 Reliability index and normalized MPFP of 4% reinforcement cross section in transverse direction.....	45
Table 5.6 Reliability index and normalized MPFP of 4% reinforcement cross section in transverse direction.....	49
Table 5.7 Reliability index and normalized MPFP of 4% reinforcement cross section in longitudinal direction	50
Table 5.8 Statistical properties of random variables for cross section of Ulsan Bridge pylon.....	52
Table 5.9 Load effect of cross section of Ulsan Bridge pylon	53
Table 5.10 Composition of wind load of Ulsan Bridge	53
Table 5.11 Reliability index and normalized MPFP of Ulsan Bridge in transverse direction	54
Table 5.12 Reliability index and normalized MPFP of Ulsan Bridge in longitudinal direction.....	55

Table 5.13 Reliability index and normalized MPFP of 2% reinforcement cross section in transverse direction.....	59
Table 5.14 Reliability index and normalized MPFP of 2% reinforcement cross section in transverse direction.....	62
Table 5.15 Reliability index and normalized MPFP of 2% reinforcement cross section in longitudinal direction	63

1. Introduction

Current bridge design code of Korea, Korean Highway Bridge Design Code (Limit State Design) (KHBDC) is reliability-based load-resistance factor design code which is based on reliability concept with statistical theory. Reliability design concept was introduced at AASHTO LRFD Bridge Design Specification in 1995 for the first time and also introduced in 2000 at Eurocode EN1990. Many studies about reliability design have done in order to get the uniform reliability level in all components of the structure.

In the design based on reliability, all components of the structure should satisfy the target reliability level proposed in the design code. Therefore designers should check all reliability level of components.

In the cable bridges, the pylons play an important role in the whole structure since they deliver external loads to foundation structures. Therefore the pylon section should be designed to ensure the target reliability level of wind load combination because the wind load combination usually dominates the pylon design.

To determine a section which secures the target reliability level, reliability analysis about the pylon section should be preceded and the section is adjusted to satisfy the target reliability. The reliability analysis method for the reinforced concrete (RC) column section was proposed by Kim, et al. (2013).

In this study, uniformly distributed reinforced concrete (UDRC) is introduced for generalizing the strength of RC column sections and the optimum sections are determined for the equivalent UDRC column sections for target reliability index.

2. Reliability Assessment of RC pylon section.

2.1 Basic Theory of Reliability Assessment

Structural reliability theory is concerned with the rational treatment of uncertainties associated with design of structures and with assessing the safety and serviceability of these structures. Reliability of a structural system is defined as the probability that the structure under consideration has a proper performance throughout its lifetime. In other words, reliability of a structure is the probability of the structure not to fail and reliability methods are used to estimate the probability of failure. Thus, reliability is expressed by following:

$$\text{Reliability} = 1 - P_f \quad (2.1)$$

where P_f is the failure probability of the structure.

Safety of a structure cannot be a deterministic value because of the uncertainties in the load effects and strengths of structural components. Civil engineering struc-

tures are designed for loads due to environmental actions like earthquakes, snow and wind or due to artificial actions like vehicle live load. These actions are exceptionally uncertain in their manifestations and their occurrence and magnitude cannot be treated deterministically. Strengths of structures also have uncertainties because of the heterogeneity of material, construction error and errors in approximation of analysis.

Variables that cannot be determined due to many different uncertainties are called random variables. Strengths of structural components and load effects are considered as random variables which don't have the same values but only can be described by possibility of having specific value. The possible values of a random variable and their associated probabilities can be explained by mathematical function which is known as a probability distribution.

Reliability of a structure is defined as failure probability of the structure. Structure designers should verify the probability of structural failure to decide whether the structure satisfies the design limit state. But to avoid the difficulty of calculate the failure probability of a structure, reliability of a structure can be checked by reliability index instead of failure probability. The reliability index, β , is the distance between the mean failure function, G , from the start defined in standard deviation units, σ_G .

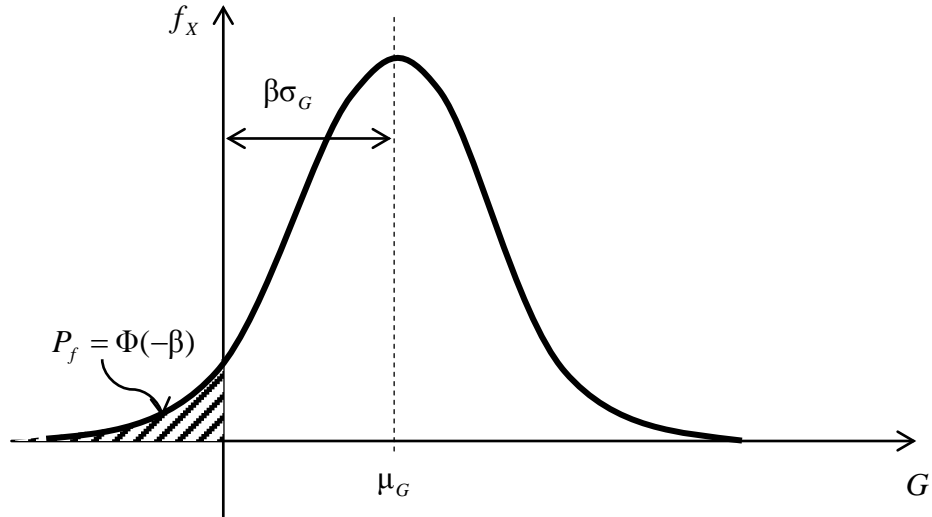


Fig. 2.1 Probabilistic concept of reliability index

In order to assess the reliability of a structure, one should define the limit state function of the structure. A limit state function is the function of random variables and it defines the limit state as the criteria that determine safety or failure of the structure. Usually the limit state function is defined such that positive values correspond to safe states and negative values correspond to failure states, therefore limit state equation is when the limit state function equals to 0, see figure 2.2. A limit state function is expressed in equation (2.2):

$$G(\mathbf{X}) = S(\mathbf{X}_s) - Q(\mathbf{X}_Q) = 0 \quad (2.2)$$

where $G(\cdot)$ denotes limit state function and $\mathbf{X} = (\mathbf{X}_s, \mathbf{X}_Q)^T = (x_1, x_2, \dots, x_n)^T$ denotes a vector of random variables. S and Q are strength and load effect of the structure,

\mathbf{X}_s and \mathbf{X}_l are random variable vectors related to strengths and loads, respectively.

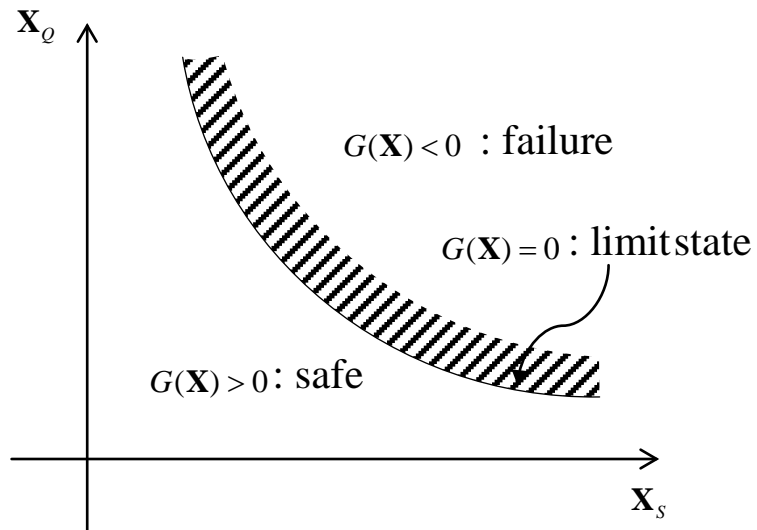


Fig. 2.2 Definition of limit state in random variable space

The relation between failure probability and reliability index of structure is shown in equation (2.3).

$$P_f(G(\mathbf{X}) < 0) = \Phi(-\beta) = 1 - \Phi(\beta) \quad (2.3)$$

where P_f denotes the failure probability and β denotes reliability index.

2.2 AFOSM with gradient projection

The failure probability of a structure can be obtained by calculating the probability that the limit state function is negative, and one can calculate it by integrating negative section of the limit state function. Hasofer & Lind (1974) defined reliability index as the smallest distance from the origin to the failure surface in the standard normal space, when the random variables are independent and normally distributed. This is illustrated in Fig. 2.3. This method is called AFOSM (Advanced First-Order Second-Moment) (Haldar and Mahadevan, 2000).

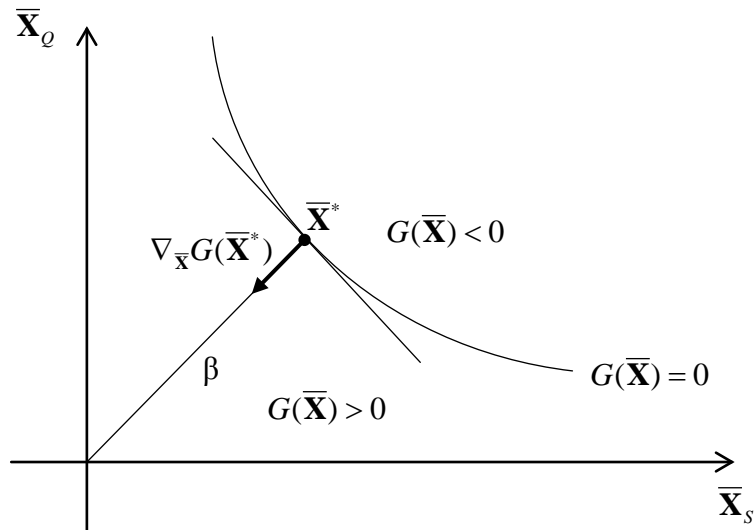


Fig. 2.3 Reliability index in standard normal space (Hasofer-Lind)

The point $\bar{\mathbf{X}}^*$ on the failure surface closet to the origin denotes most probable failure point (MPFP). The reliability index is thus defined by the optimization problem:

$$\text{Min}_{\bar{\mathbf{X}}} \beta^2 = \|\bar{\mathbf{X}}\|_2^2 \quad \text{subject to} \quad G(\bar{\mathbf{X}}) = G(\mathbf{X}) = 0 \quad (2.4)$$

(2.5) is the equation of the tangential plane which includes the point $\bar{\mathbf{X}}^*$ in standard normal space:

$$G(\bar{\mathbf{X}}^*) + \nabla_{\bar{\mathbf{X}}} G(\bar{\mathbf{X}}^*) \cdot (\bar{\mathbf{X}} - \bar{\mathbf{X}}^*) = 0 \quad (2.5)$$

where $\nabla_{\bar{\mathbf{X}}}$ is a gradient operator for standard normal variable and the first term is to be 0 because the point $\bar{\mathbf{X}}^*$ is on the limit state equation. Distance from origin to tangential surface β can be written:

$$\beta = \frac{-\nabla_{\bar{\mathbf{X}}} G(\bar{\mathbf{X}}^*) \cdot \bar{\mathbf{X}}^*}{\|\nabla_{\bar{\mathbf{X}}} G(\bar{\mathbf{X}}^*)\|_2} \quad (2.6)$$

where $\|\cdot\|_2$ means 2-norm of vectors.

Relation of gradient between original random variable \mathbf{X} and its equivalent standard normal variable $\bar{\mathbf{X}}$ is shown in (2.7)

$$\nabla G_{\bar{\mathbf{X}}}(\bar{\mathbf{X}}) = \nabla G_{\mathbf{X}}(\mathbf{X}) \cdot J_{\mathbf{X}\bar{\mathbf{X}}} \quad (2.7 \text{ a})$$

$$G_{\mathbf{X}}(\mathbf{X}) = G_{\bar{\mathbf{X}}}(\bar{\mathbf{X}}) \quad (2.7 \text{ b})$$

$J_{\mathbf{X}\bar{\mathbf{X}}}$ denotes Jacobian when send \mathbf{X} to $\bar{\mathbf{X}}$.

Solution of optimization problem (2.4) is MPFP and one could calculate it by using iterative scheme if the limit state equation is nonlinear equation. The following shows a first order Taylor approximation of limit state equation at previous MPFP point in standard normal space.

$$G(\bar{\mathbf{X}}_{k+1}) \approx G(\bar{\mathbf{X}}_k) + \nabla_{\bar{\mathbf{X}}} G(\bar{\mathbf{X}}_k) \cdot (\bar{\mathbf{X}}_{k+1} - \bar{\mathbf{X}}_k) = 0 \quad (2.8)$$

where k is iteration number and $\bar{\mathbf{X}}_{k+1}$ is MPFP in current iteration.

At the MPFP $\bar{\mathbf{X}}_{k+1}$ it is seen that the following relation must be fulfilled:

$$\bar{\mathbf{X}}_{k+1} = -\kappa_{k+1} \nabla G_{\bar{\mathbf{X}}}(\bar{\mathbf{X}}_k) \quad (2.9)$$

where κ_{k+1} is undetermined coefficient and can be calculated by using the condition that point $\bar{\mathbf{X}}_{k+1}$ is on the limit state equation. Liu & Der Kiureghian (1991) proposed gradient projection method based on Newton-Raphson method to make equation (2.9) always satisfy the limit state equation.

$$G(-\kappa_{k+1} \nabla_{\bar{\mathbf{X}}} G(\bar{\mathbf{X}}_k)) = 0 \quad (2.10)$$

When the limit state equation is non-linear equation, another iterative calculation is necessary for determination of κ_{k+1} .

$$(\kappa_{k+1})_{p+1} = (\kappa_{k+1})_p + \Delta\kappa \quad (2.11)$$

where $p+1$ is the number of inner iteration for determining κ_{k+1} and application of (2.11) and (2.10) gives:

$$\begin{aligned} G(-(\kappa_{k+1})_{p+1} \cdot \nabla_{\bar{\mathbf{X}}} G(\bar{\mathbf{X}}_k)) &\approx G(-(\kappa_{k+1})_p \cdot \nabla_{\bar{\mathbf{X}}} G(\bar{\mathbf{X}}_k)) + \left. \frac{\partial G}{\partial \bar{\mathbf{X}}} \frac{\partial \bar{\mathbf{X}}}{\partial \kappa} \right|_{\kappa=\kappa_p} \cdot \Delta\kappa \\ &= G(-(\kappa_{k+1})_p \cdot \nabla_{\bar{\mathbf{X}}} G(\bar{\mathbf{X}}_k)) - \nabla_{\bar{\mathbf{X}}} G(-(\kappa_{k+1})_p \cdot \nabla_{\bar{\mathbf{X}}} G(\bar{\mathbf{X}}_k)) \cdot \nabla_{\bar{\mathbf{X}}} G(\bar{\mathbf{X}}_k) \cdot \Delta\kappa \\ &= 0 \end{aligned} \quad (2.12)$$

Therefore one can obtain $\Delta\kappa$ from (2.12)

$$\Delta\kappa = \frac{G(-(\kappa_{k+1})_p \cdot \nabla_{\bar{\mathbf{X}}} G(\bar{\mathbf{X}}_k))}{\nabla_{\bar{\mathbf{X}}} G(-(\kappa_{k+1})_p \cdot \nabla_{\bar{\mathbf{X}}} G(\bar{\mathbf{X}}_k)) \cdot \nabla_{\bar{\mathbf{X}}} G(\bar{\mathbf{X}}_k)} \quad (2.13)$$

In the inner iteration, initial value of κ_{k+1} is defined by (2.14).

$$(\kappa_{k+1})_0 = -\frac{\nabla_{\bar{\mathbf{X}}}G(\bar{\mathbf{X}}_k) \cdot \bar{\mathbf{X}}_k}{\nabla_{\bar{\mathbf{X}}}G(\bar{\mathbf{X}}_k) \cdot \nabla_{\bar{\mathbf{X}}}G(\bar{\mathbf{X}}_k)} \quad (2.14)$$

One can determine κ by inner iteration (2.10) - (2.14) and then MPFP value can be determined by outer iteration (2.9), thus the reliability index can be estimated.

2.3 Rackwitz-Fiessler transformation

One can use Hasofer & Lind method for calculation of reliability index when all random variables are independent of each other and normally distributed. Since random variables are not generally normally distributed, it is necessary to establish a transformation to standardized normally distributed variables in order to determine a measure of the reliability with non-normally distributed variables.

Rackwitz & Fiessler (1978) suggested a method for transforming a non-normal variable into an equivalent normal variable by estimating the parameters of the equivalent normal distribution. They assumed the cumulative distribution functions and the probability density functions of the actual variables and the equivalent normal variables should be equal at the MPFP on the failure surface (2.5).

$$\frac{1}{\sigma_X^{eq}} \varphi\left(\frac{x_i - \mu_X^{eq}}{\sigma_X^{eq}}\right) = f_i(x_i) \quad (2.15a)$$

$$\Phi\left(\frac{x_i - \mu_X^{eq}}{\sigma_X^{eq}}\right) = F_i(x_i) \quad (2.15b)$$

F_i and f_i are the non-normal cumulative distribution and density functions of X_i ; and Φ and φ are the cumulative distribution and density function of the standard normal variate, respectively. The mean value, μ_X^{eq} , and standard deviation, σ_X^{eq} , of the equivalent normal variables are shown in (2.16)

$$\begin{aligned} \mu_X^{eq} &= x_i - \sigma_X^{eq} \Phi^{-1}(F_i(x_i)) \\ \sigma_X^{eq} &= \frac{\varphi(\Phi^{-1}(F_i(x_i)))}{f_i(x_i)} \end{aligned} \quad (2.16)$$

One can transform original MPFP into normally distributed variables by Rackwitz-Fiessler transformation and then calculate next MPFP through inner iteration. After obtaining new MPFP in normal space, it can be converted to the one in original space by reverse Rackwitz-Fiessler transformation

Non-normal variables should be transformed into normal variables and normalized with expected value 0 and standard deviation 1 by (2.17), therefore Jacobian value in (2.6a) is determined by equivalent standard deviation, $J_{X_i \bar{X}_i} = \sigma_{X_i}^{eq}$.

$$\bar{X}_i = \frac{X_i - \mu_{X_i}^{eq}}{\sigma_{X_i}^{eq}} \quad (2.17)$$

During the iteration procedures, iteration can be terminated when the difference of MPFPs in every step satisfies the convergence criteria and reliability index is decided by MPFP at the last step. This reliability analysis by Hasofer-Lind method based on Rackwitz-Fiessler transformation is called Hasofer-Lind Rackwitz-Fiessler (HL-RF) algorithm (Liu and Der Kiureghian, 1991).

3. Uniformly Distributed Reinforcement

3.1 Definition of Uniformly Distributed Reinforcement

In this study, RC column with uniformly distributed reinforcement is defined as a concrete column which contains reinforcement all over the section. It is assumed that rebar is separated in small pieces like powder and distributed uniformly in the section. Therefore a general RC column section and equivalent uniformly distributed reinforced concrete column (UDRC column) section have the same quantity of total reinforcement. Strength of UDRC column is defined as combination of reinforcement strength and concrete strength with the reinforcement ratio. It is possible to simplify the computation to find the target section because it can be decided with total section area and reinforcement ratio.

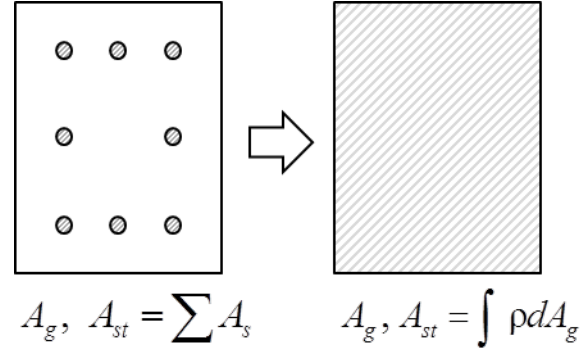
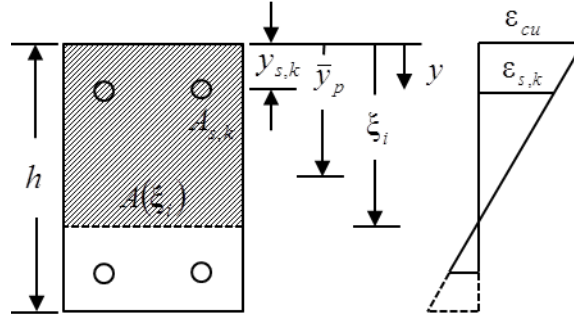


Fig. 3.1 Equivalent uniformly distributed reinforced concrete

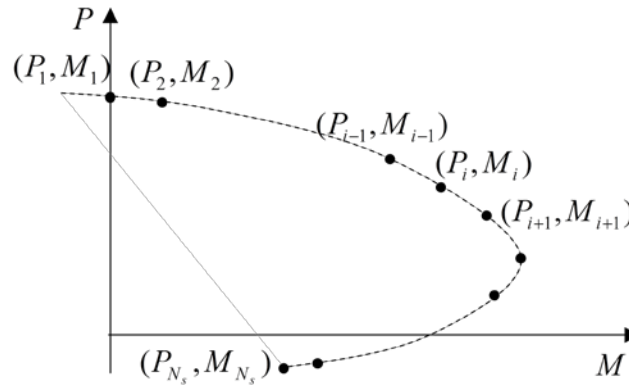
3.2 PMID of Uniformly Distributed Reinforced Concrete Column

When reinforced concrete members are subject to combined compressive axial load and bending, the strength is defined by the P-M interaction diagram (PMID). A PMID consists of several sample points which are determined by location of sectional neutral axis. Axial and moment strengths at an arbitrary neutral axis ξ are determined by (3.1) in general reinforced concrete member.

$$\begin{aligned}
 P &= \int_{A_g(\xi)} \sigma_c dA_g - \sum_{k=1}^{m_c} A_{s,k} \sigma_{c,k} + \sum_{k=1}^m A_{s,k} \sigma_{s,k} \\
 M &= \int_{A_g(\xi)} (\bar{y}_p - y) \sigma_c dA_g - \sum_{k=1}^{m_c} (\bar{y}_p - y_k) A_{s,k} \sigma_{c,k} + \sum_{k=1}^m (\bar{y}_p - y_k) A_{s,k} \sigma_{s,k}
 \end{aligned} \tag{3.1}$$



(a) Definition of geometric properties



(b) Sample points of PMID

Fig. 3.2 Typical cross section of an RC column and PMID

As shown in equation (3.1), strength of general RC column section is expressed by integration term of concrete strength from compression face to neutral axis and sum of steel strength at every location of reinforcement. Strength of equivalent UDRC column section is shown in (3.2). Compared to (3.1), equation (3.2) is simplified with gross section, concrete and steel strengths because reinforcement place uniformly all over the section.

$$\begin{aligned}
P &= \int_{A_g(\xi)} \sigma_c dA \times (1-\rho) + \int_{A_g} \sigma_s dA \times \rho \\
M &= \int_{A_g(\xi)} (\bar{y}_p - y) \sigma_c dA \times (1-\rho) + \int_{A_g} (\bar{y}_p - y) \sigma_s dA \times \rho
\end{aligned} \tag{3.2}$$

Here, plastic centroid coincides with centroid of area because of the uniformly distributed reinforcement.

$$\bar{y}_p = \frac{\sigma_{cu} A_g \bar{y}_c (1-\rho) + f_y A_g \bar{y}_c \rho}{\sigma_{cu} A_g (1-\rho) + f_y A_g \rho} = \bar{y}_c = \frac{\int_{A_g} y dA}{A_g} \tag{3.3}$$

Axial and moment strength at i -th sample point is calculated by numerical integration (3.4).

$$\begin{aligned}
P_i &\approx \frac{A_g}{N_l} \sum_{k=0}^{i-1} \sigma_{c,k+1/2} (1-\rho) + \frac{A_g}{N_l} \sum_{k=0}^{N_s-1} \sigma_{s,k+1/2} \rho \\
M_i &\approx \frac{A_g}{N_l} \sum_{k=0}^{i-1} (\bar{y}_p - y_{k+1/2}) \sigma_{c,k+1/2} (1-\rho) + \frac{A_g}{N_l} \sum_{k=0}^{N_s-1} (\bar{y}_p - y_{k+1/2}) \sigma_{s,k+1/2} \rho \\
&= \bar{y}_p P_i - \frac{A_g}{N_l} \sum_{k=0}^{i-1} y_{k+1/2} \sigma_{c,k+1/2} (1-\rho) + \frac{A_g}{N_l} \sum_{k=0}^{N_s-1} y_{k+1/2} \sigma_{s,k+1/2} \rho
\end{aligned} \tag{3.4}$$

Following shows the stress of steel and concrete material according to strain. Effective compression coefficient is denoted α_{cc} and is applied 0.85.

$$\sigma_s = \begin{cases} E_s \varepsilon_s & \varepsilon_s < \varepsilon_y \\ f_y & \varepsilon_s \geq \varepsilon_y \end{cases} \quad (3.5 \text{ a})$$

$$\sigma_c = \begin{cases} \alpha_{cc} f_{ck} (1 - (1 - \varepsilon_c / \varepsilon_{co})^n) & 0 \leq \varepsilon_c < \varepsilon_{co} \\ \alpha_{cc} f_{ck} & \varepsilon_{co} \leq \varepsilon_c \leq \varepsilon_{cu} \end{cases} \quad (3.5 \text{ b})$$

Determination coefficient of stress-strain curve is shown in (3.6)

$$n = \begin{cases} 2.0 & f_{ck} \leq 40 \text{ MPa} \\ 1.2 + 1.5 \left(\frac{100 - f_{ck}}{60} \right)^4 \leq 2.0 & f_{ck} > 40 \text{ MPa} \end{cases}$$

$$\varepsilon_{co} = \begin{cases} 0.002 & f_{ck} \leq 40 \text{ MPa} \\ 0.02 + \frac{f_{ck} - 40}{100000} & f_{ck} > 40 \text{ MPa} \end{cases} \quad (3.6)$$

$$\varepsilon_{cu} = \begin{cases} 0.0033 & f_{ck} \leq 40 \text{ MPa} \\ 0.0033 - \frac{f_{ck} - 40}{100000} & f_{ck} > 40 \text{ MPa} \end{cases}$$

Maximum compressive strain, $\varepsilon(0)$, and strain at y from compression face, $\varepsilon(y)$, are shown in (3.7).

$$\varepsilon(0) = \begin{cases} \varepsilon_{cu} & 0 < \xi \leq h \\ \varepsilon_{cu} \frac{\varepsilon_{co}}{\left(1 - \frac{h}{\xi}\right)\varepsilon_{cu} + \frac{h}{\xi}\varepsilon_{co}} & \xi > h \end{cases} \quad (3.7 \text{ a})$$

$$\varepsilon(y) = \left(1 - \frac{y}{\xi}\right)\varepsilon(0) \quad (3.7 \text{ b})$$

3.3 Reliability Assessment of RC pylon cross section

An important step in reliability analysis is to decide which quantities should be modelled by random variables and to define the limit state function. As shown in Fig. 3.3 strength of RC column and load effect can be expressed on PMID. The load point inside the P-M curve represents the structural component is in a safe state, otherwise the load point outside the P-M curve means the component in a failure state. Therefore the load point on the P-M curve is defined as limit state and PMID can be defined as a limit state equation.

$$\begin{aligned} \Phi(\mathbf{F}, \mathbf{B}) &= 0 \\ \mathbf{F} &= (P, M)^T = \mathbf{C}\mathbf{q} \end{aligned} \quad (3.8)$$

Here, \mathbf{F} is the internal force vector representing the load effects of external load components, and \mathbf{B} is the curve parameter vector of the P-M interaction diagram. \mathbf{C} and \mathbf{q} are the load effect matrix and load parameter vector, respectively.

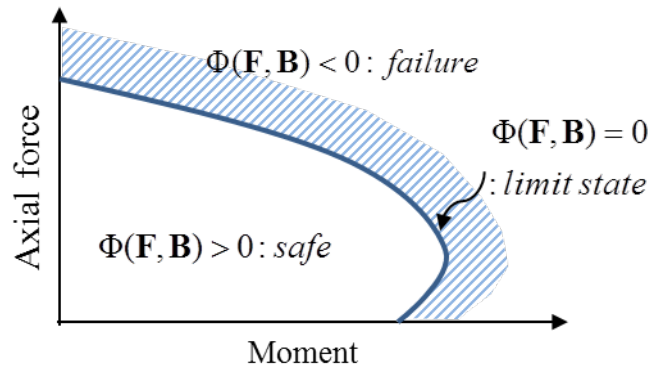


Fig. 3.3 Limit state function of RC columns

For reliability analysis, one should be able to calculate sensitivity of limit state equation, that is, derivatives of limit state equation should exist. Since derivatives of sample points cannot be defined in (3.1) or (3.2), a curve which connects two adjacent points should be redefined as a continuous equation by approximating it to cubic spline (Kim, et al., 2013).

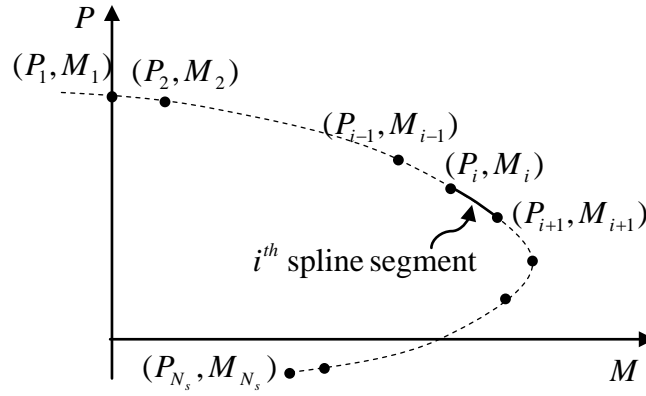


Fig. 3.4 PMID approximated by cubic spline

$$\Phi_i = \Phi_i(P, M, \mathbf{B}_i) = a_i + b_i(P - P_i) + c_i(P - P_i)^2 + d_i(P - P_i)^3 - M = 0$$

$$\Phi(P, M, \mathbf{B}) = \bigcup_{i=1}^{N_s-1} \Phi_i(P, M, \mathbf{B}_i) \quad (i = 1, \dots, N_s - 1) \quad (3.9)$$

$$\mathbf{B}_i = (a_i, b_i, c_i, d_i)^T$$

Load variables and strength variables are random variables which have variability by uncertainties.

$$\mathbf{X} = (\mathbf{q}, \mathbf{s})^T \quad (3.10)$$

$$\mathbf{q} = (DC_p, DC_c, DC_g, DW, WS, LL, EQ, \dots)^T \quad (3.11)$$

$$\mathbf{s} = (f_{ck}, f_y, E_s, A_g, A_{s,1}, \dots, A_{s,m}, y_{s,1}, \dots, y_{s,m})^T \quad (3.12 \text{ a})$$

$$\mathbf{s} = (f_{ck}, f_y, E_s, A_g, A_s)^T \quad (3.12 \text{ b})$$

In the equation (3.10), \mathbf{q} and \mathbf{s} denote load and strength parameters, respectively. Load parameters include dead load, wind load, live load, earthquake load and etc. Strength parameters represent material properties and geometric properties of a cross section. Material properties include compressive strength of concrete, f_{ck} , yield strength of the reinforcement, f_y and the Young's modulus of the reinforcement, E_s . The geometric properties consist of the gross area of a cross section and information of reinforcement. When a RC column section has general reinforcement, information of reinforcement is the area and position of each reinforcing bar (3.6a). In the case of UDRC column section, the information of reinforcement is the gross area of whole reinforcement (3.6b).

The followings are i -th segment of cubic spline and its derivatives:

$$g_i(P) = M = a_i + b_i(P - P_i) + c_i(P - P_i)^2 + d_i(P - P_i)^3 \quad (3.13 \text{ a})$$

$$(i = 1, \dots, N_s)$$

$$g'_i(P) = b_i + 2c_i(P - P_i) + 3d_i(P - P_i)^2 \quad (3.13 \text{ b})$$

$$g''_i(P) = 2c_i + 6d_i(P - P_i) \quad (3.13 \text{ c})$$

The unknown coefficients of each spline segment are determined through the continuity requirements at the boundary between two adjacent spline segments. The coefficients of each spline are defined as follow:

$$a_i = M_i \quad (i = 1, \dots, N_s) \quad (3.14)$$

$$\mathbf{c} = \mathbf{p}^{-1} \mathbf{r} \quad (3.15)$$

$$\mathbf{c} = (c_2, c_3, \dots, c_{N_s-1})^T \quad (3.15 \text{ a})$$

$$\mathbf{p} = \begin{bmatrix} 2(p_1 + p_2) & p_2 & & & & \\ p_2 & 2(p_2 + p_3) & p_3 & & & \\ & & \ddots & \ddots & \ddots & \\ & & & & p_{N_s-2} & 2(p_{N_s-2} + p_{N_s-1}) \end{bmatrix} \quad (3.15 \text{ b})$$

$$\mathbf{r} = \begin{pmatrix} 3\left(\frac{a_4 - a_3}{p_3} - \frac{a_3 - a_2}{p_2}\right) \\ 3\left(\frac{a_5 - a_4}{p_4} - \frac{a_4 - a_3}{p_3}\right) \\ \vdots \\ 3\left(\frac{a_{N_s-1} - a_{N_s-2}}{p_{N_s-2}} - \frac{a_{N_s-2} - a_{N_s-3}}{p_{N_s-3}}\right) \end{pmatrix} \quad (3.15 \text{ c})$$

where $p_{i-1} = P_i - P_{i-1}$. The coefficients c_i are obtained by solving equation (3.15) with (3.15 a, b, c). The boundary condition $c_1 = c_{N_s} = 0$ is imposed based on the continuity of second derivative condition, $d^2g_i/dP^2 = 0$ at $P = P_1, P_{N_s}$. The

other coefficients b_i (3.16) and d_i (3.17) can be solved by substituting a_i and c_i into (3.13) and continuity conditions.

$$b_i = \frac{a_{i+1} - a_i}{p_i} - \frac{2c_i + c_{i+1}}{3} p_i \quad (i = 1, \dots, N_s - 1) \quad (3.16)$$

$$d_i = \frac{c_{i+1} - c_i}{3p_i} \quad (i = 1, \dots, N_s - 1) \quad (3.17)$$

The sensitivities of the limit state equation with respect to the random variables are calculated by the direct differentiation of the P-M interaction diagram using chain-rule.

$$\begin{aligned} \begin{bmatrix} \frac{\partial \Phi}{\partial \mathbf{q}} \\ \frac{\partial \Phi}{\partial \mathbf{s}} \end{bmatrix} &= \begin{bmatrix} \frac{\partial \Phi}{\partial \mathbf{F}} \frac{\partial \mathbf{F}}{\partial \mathbf{q}} & \frac{\partial \Phi}{\partial \mathbf{B}} \frac{\partial \mathbf{B}}{\partial \mathbf{q}} \\ \frac{\partial \Phi}{\partial \mathbf{F}} \frac{\partial \mathbf{F}}{\partial \mathbf{s}} & \frac{\partial \Phi}{\partial \mathbf{B}} \frac{\partial \mathbf{B}}{\partial \mathbf{s}} \end{bmatrix} = \begin{bmatrix} \left(\frac{\partial \mathbf{F}}{\partial \mathbf{q}}\right)^T & \left(\frac{\partial \mathbf{B}}{\partial \mathbf{q}}\right)^T \\ \left(\frac{\partial \mathbf{F}}{\partial \mathbf{s}}\right)^T & \left(\frac{\partial \mathbf{B}}{\partial \mathbf{s}}\right)^T \end{bmatrix} \begin{bmatrix} \frac{\partial \Phi}{\partial \mathbf{F}} \\ \frac{\partial \Phi}{\partial \mathbf{B}} \end{bmatrix} = \mathbf{Q} \begin{bmatrix} \frac{\partial \Phi}{\partial \mathbf{F}} \\ \frac{\partial \Phi}{\partial \mathbf{B}} \end{bmatrix} \\ \mathbf{Q} &= \begin{bmatrix} \mathbf{C}^T & 0 \\ 0 & \left(\frac{\partial \mathbf{B}}{\partial \mathbf{s}}\right)^T \end{bmatrix} \end{aligned} \quad (3.18)$$

As the coefficients of the PMID and the internal forces are independent to the load parameters and the strength parameters, respectively, the off-diagonal entries of matrix \mathbf{Q} is vanish. The sensitivities of P-M interaction diagram are followed:

$$\frac{\partial \Phi_i}{\partial \mathbf{F}} = \begin{pmatrix} \frac{\partial \Phi_i}{\partial P} \\ \frac{\partial \Phi_i}{\partial M} \end{pmatrix} = \begin{pmatrix} b_i + 2c_i(P - P_i) + 3d_i(P - P_i)^2 \\ -1 \end{pmatrix} \quad (3.19 \text{ a})$$

$$\frac{\partial \Phi_i}{\partial \mathbf{B}} = \begin{pmatrix} 1 \\ (P - P_i) \\ (P - P_i)^2 \\ (P - P_i)^3 \end{pmatrix} \quad (3.19 \text{ b})$$

The sensitivities of curve parameters with respect to strength parameter are shown in (3.20), when the total number of strength parameter is N_p .

$$\begin{aligned} \frac{\partial \mathbf{B}}{\partial \mathbf{s}} &= \frac{\partial \mathbf{B}_i}{\partial s_j} = \left(\frac{\partial a_i}{\partial s_j}, \frac{\partial b_i}{\partial s_j}, \frac{\partial c_i}{\partial s_j}, \frac{\partial d_i}{\partial s_j} \right)^T, \quad (j = 1, \dots, N_p) \\ \frac{\partial a_i}{\partial s_j} &= \frac{\partial M_i}{\partial s_j}, \quad (i = 1, \dots, N_s) \\ \frac{\partial \mathbf{c}}{\partial s_j} &= \mathbf{p}^{-1} \left(\frac{\partial \mathbf{r}}{\partial s_j} - \frac{\partial \mathbf{p}}{\partial s_j} \mathbf{c} \right) \\ \frac{\partial r_i}{\partial s_j} &= 3 \left[\frac{1}{p_i} \left(\frac{\partial M_{i+1}}{\partial s_j} - \frac{\partial M_i}{\partial s_j} \right) - \frac{M_{i+1} - M_i}{p_i^2} \frac{\partial p_i}{\partial s_j} \right. \\ &\quad \left. - \frac{1}{p_{i-1}} \left(\frac{\partial M_i}{\partial s_j} - \frac{\partial M_{i-1}}{\partial s_j} \right) + \frac{M_i - M_{i-1}}{p_{i-1}^2} \frac{\partial p_{i-1}}{\partial s_j} \right] \\ \frac{\partial b_i}{\partial s_j} &= \left(\frac{\partial a_{i+1}}{\partial s_j} - \frac{\partial a_i}{\partial s_j} \right) \frac{1}{p_i} - \frac{a_{i+1} - a_i}{p_i^2} \frac{\partial p_i}{\partial s_j} \\ &\quad - \frac{1}{3} \left(2 \frac{\partial c_i}{\partial s_j} + \frac{\partial c_{i+1}}{\partial s_j} \right) p_i - \frac{2c_i + c_{i+1}}{3} \frac{\partial p_i}{\partial s_j} \\ \frac{\partial d_i}{\partial s_j} &= \frac{1}{3p_i} \left(\frac{\partial c_{i+1}}{\partial s_j} - \frac{\partial c_i}{\partial s_j} \right) - \frac{c_{i+1} - c_i}{3p_i^2} \frac{\partial p_i}{\partial s_j} \end{aligned} \quad (3.20)$$

The sensitivities of axial strength and moment with respect to material parameters and geometric parameters are followed in (3.21)

$$\begin{aligned}
\frac{\partial P_i}{\partial f_{ck}} &= \frac{A_g}{N_l} \sum_{k=0}^{i-1} \frac{\partial \sigma_{c,k+1/2}}{\partial f_{ck}} (1-\rho) \\
\frac{\partial P_i}{\partial f_y} &= \frac{A_g}{N_l} \sum_{k=0}^{N_s-1} \frac{\partial \sigma_{s,k+1/2}}{\partial f_{ck}} \rho \\
\frac{\partial P_i}{\partial E_s} &= \frac{A_g}{N_l} \sum_{k=0}^{N_s-1} \frac{\partial s_{s,k+1/2}}{\partial E_s} \rho \\
\frac{\partial P_i}{\partial A_g} &= \frac{1}{N_l} \sum_{k=0}^{i-1} \sigma_{c,k+1/2} (1-\rho) + \frac{1}{N_l} \sum_{k=0}^{N_s-1} \sigma_{s,k+1/2} \rho \\
\frac{\partial P_i}{\partial A_s} &= \frac{\partial P_i}{\partial \rho} \frac{\partial \rho}{\partial A_s} = -\frac{1}{N_l} \sum_{k=0}^{i-1} \sigma_{c,k+1/2} + \frac{1}{N_l} \sum_{k=0}^{N_s-1} \sigma_{s,k+1/2} \\
\frac{\partial M_i}{\partial f_{ck}} &= \frac{\partial \bar{y}_p}{\partial f_{ck}} P_i + \bar{y}_p \frac{\partial P_i}{\partial f_{ck}} - \frac{A_g}{N_l} \sum_{k=0}^{i-1} y_{k+1/2} \frac{\partial \sigma_{c,k+1/2}}{\partial f_{ck}} (1-\rho) \\
\frac{\partial M_i}{\partial f_y} &= \frac{\partial \bar{y}_p}{\partial f_y} P_i + \bar{y}_p \frac{\partial P_i}{\partial f_y} - \frac{A_g}{N_l} \sum_{k=0}^{N_s-1} y_{k+1/2} \frac{\partial \sigma_{s,k+1/2}}{\partial f_{ck}} \rho \\
\frac{\partial M_i}{\partial E_s} &= \frac{\partial \bar{y}_p}{\partial E_s} P_i + \bar{y}_p \frac{\partial P_i}{\partial E_s} - \frac{A_g}{N_l} \sum_{k=0}^{N_s-1} y_{k+1/2} \frac{\partial s_{s,k+1/2}}{\partial E_s} \rho \\
\frac{\partial M_i}{\partial A_g} &= \frac{\partial \bar{y}_p}{\partial A_g} P_i + \bar{y}_p \frac{\partial P_i}{\partial A_g} - \frac{1}{N_l} \sum_{k=0}^{i-1} y_{k+1/2} \sigma_{c,k+1/2} (1-\rho) - \frac{1}{N_l} \sum_{k=0}^{N_s-1} y_{k+1/2} \sigma_{s,k+1/2} \rho \\
\frac{\partial M_i}{\partial A_s} &= \frac{\partial M_i}{\partial \rho} \frac{\partial \rho}{\partial A_s} = \frac{\partial \bar{y}_p}{\partial A_s} P_i + \bar{y}_p \frac{\partial P_i}{\partial A_s} + \frac{1}{N_l} \sum_{k=0}^{i-1} y_{k+1/2} \sigma_{c,k+1/2} - \frac{1}{N_l} \sum_{k=0}^{N_s-1} y_{k+1/2} \sigma_{s,k+1/2} \\
\frac{\partial \bar{y}_p}{\partial f_{ck}} &= 0, \quad \frac{\partial \bar{y}_p}{\partial f_y} = 0, \quad \frac{\partial \bar{y}_p}{\partial E_s} = 0, \quad \frac{\partial \bar{y}_p}{\partial A} = 0, \quad \frac{\partial \bar{y}_p}{\partial \rho} = 0
\end{aligned} \tag{3.21}$$

Partial derivatives are defined as following.

$$\begin{aligned}
\frac{\partial \sigma_{c,k}}{\partial f_{ck}} &= \alpha_{cc} \left[1 - \left(1 - \frac{\varepsilon_c}{\varepsilon_{co}} \right)^n \right] + \alpha_{cc} f_{ck} \left(1 - \frac{\varepsilon_c}{\varepsilon_{co}} \right)^n \left[\ln \left(1 - \frac{\varepsilon_c}{\varepsilon_{co}} \right) \frac{\partial n}{\partial f_{ck}} \right. \\
&\quad \left. - \frac{n}{\varepsilon_{co} - \varepsilon_c} \frac{\partial \varepsilon_c}{\partial f_{ck}} + \frac{n \varepsilon_c}{(\varepsilon_{co} - \varepsilon_c) \varepsilon_{co}} \frac{\partial \varepsilon_{co}}{\partial f_{ck}} \right] \quad \varepsilon_{co} \leq \varepsilon_c \leq \varepsilon_{ci} \\
\frac{\partial n}{\partial f_{ck}} &= \begin{cases} 0 & f_{ck} < 48.725 \text{ MPa} \\ -\frac{1}{10} \left(\frac{100 - f_{ck}}{60} \right)^3 & f_{ck} \geq 48.725 \text{ MPa} \end{cases} \\
\frac{\partial \varepsilon_{co}}{\partial f_{ck}} &= \begin{cases} 0 & f_{ck} < 40 \text{ MPa} \\ \frac{1}{100000} & f_{ck} \geq 40 \text{ MPa} \end{cases} \\
\frac{\partial \varepsilon_c}{\partial f_k} &= \left(1 - \frac{y}{\xi} \right) \frac{\partial \varepsilon(0)}{\partial f_{ck}} \\
\frac{\partial \varepsilon(0)}{\partial f_{ck}} &= \begin{cases} \frac{\partial \varepsilon_{cu}}{\partial f_{ck}} & \xi < h \\ \frac{\varepsilon_{co}^2 \frac{h}{\xi} \frac{\partial \varepsilon_{cu}}{\partial f_{ck}} + \varepsilon_{cu}^2 \left(1 - \frac{h}{\xi} \right) \frac{\partial \varepsilon_{co}}{\partial f_{ck}}}{\left[\left(1 - \frac{h}{\xi} \right) \varepsilon_{cu} + \frac{h}{\xi} \varepsilon_{co} \right]^2} & \xi > h \end{cases} \\
\frac{\partial \varepsilon_{cu}}{\partial f_{ck}} &= \begin{cases} 0 & f_{ck} < 40 \text{ MPa} \\ -\frac{1}{100000} & f_{ck} \geq 40 \text{ MPa} \end{cases} \\
\frac{\partial \sigma_{s,k}}{\partial f_y} &= \begin{cases} -1 & \varepsilon_s \leq -\varepsilon_y \\ 0 & -\varepsilon_y < \varepsilon_s < \varepsilon_y \\ 1 & \varepsilon_s \geq \varepsilon_y \end{cases} \\
\frac{\partial \sigma_{s,k}}{\partial E_s} &= \begin{cases} 0 & \varepsilon_s \leq -\varepsilon_y \\ \varepsilon_s & -\varepsilon_y < \varepsilon_s < \varepsilon_y \\ 0 & \varepsilon_s \geq \varepsilon_y \end{cases}
\end{aligned} \tag{3.22}$$

3.4 Comparison of Reliability Index for discrete and uniformly distributed reinforced RC column

To check the validity of UDRC assumption as a substitution of general reinforced concrete, the following example is considered: a simple rectangular section with symmetrically placed reinforcing bars. Reliability analysis is carried out for example section and for equivalent UDRC section and the results are compared.

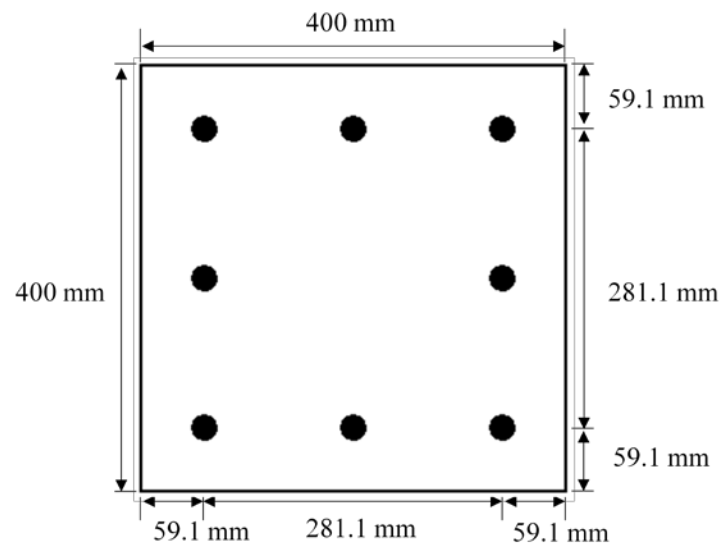


Fig. 3.5 Cross section of example RC column

The example is 400mm×400mm square section having 8-D19 rebar and the properties of load and strength are presented in table 3.1 and table 3.2.

Table 3.1 Statistical properties of random variables in example section

Random variable	Nominal value	Bias factor	COV	Distribution type	
Material properties	f_{ck}	27 MPa	1.150	0.100	Lognormal
	f_y	400 MPa	1.150	0.080	Lognormal
	E_s	200 GPa	1.000	0.060	Lognormal
Geometric properties	e_s	0.0 mm	1.000	-	Normal
	A_s	2,272 mm ² ($\rho = 0.0142$)	1.000	0.015	Normal
	A_{gt}	160,000 mm ²	1.010	0.000	Normal
Load parameters	DC_p	1.00	1.050	0.10	Normal
	DC_g	1.00	1.030	0.08	Normal
	DW	1.00	1.000	0.25	Normal
	WS	1.00	1.123	0.29	Extreme-type I

Table 3.2 External load effect of example section

Total nominal load effects	Load effect matrix				Deterministic values	
	DC_p	DC_g	DW	WS		
P_q (MN)	1.05	0.40	0.50	0.10	0.05	0.00
M_q (MN·m)	0.03	0.01	0.05	-0.03	0.00	0.00

Table 3.3 presents the reliability indices and normalized MPFPs. Fig. 3.6 show the failure points and the limit P-M interaction diagrams for the example section and equivalent UDRC section. The x-axis and y-axis represent bending moment and axial force normalized by nominal value of external load, respectively. The relative er-

ror of two analysis result is less than 1% and UDRC section seems to represent well the P-M interaction diagram.

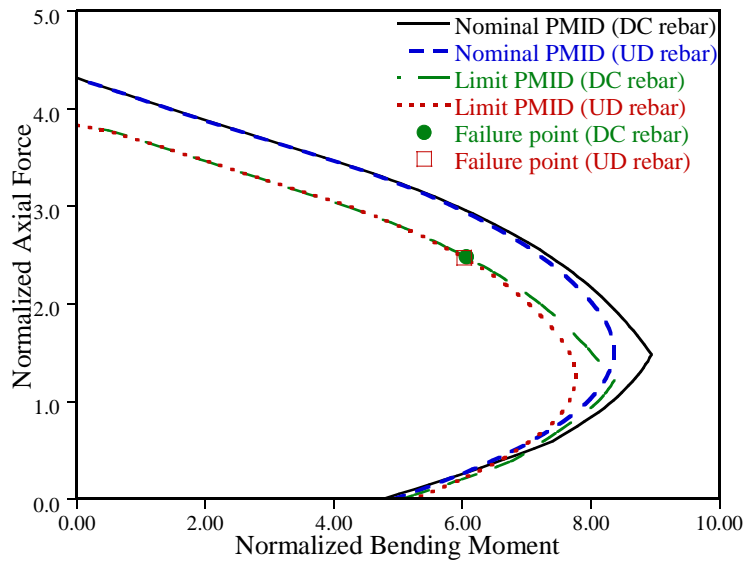


Fig. 3.6 Nominal and limit PMIDs and MPFPs of example section

Table 3.3 Reliability index and normalized MPFP of example section

rebar	Relia- bility index	Normalized MPFP									
		Material properties			Geometric proper- ties				Load parameters		
		f_{ck}	f_y	E_s	$(e_s)_{avg.}$	A_s	A_{gt}	DC_p	DC_g	DW	WS
DC	7.76	0.85	1.09	1.00	0.00	1.00	1.01	1.10	1.02	1.03	4.02
UD	7.72	0.85	1.10	1.00	-	1.00	1.01	1.10	1.01	1.02	4.01

4. Optimization of pylon section for Target Reliability.

An optimum section which satisfies the target reliability level is determined by a series of reliability analysis and updating the section steps. A column section has two independent reliabilities in transverse and longitudinal directions. Therefore one can decide the section for target reliability level for one direction or both of two directions as occasion demands.

4.1 General method

The equation for determination of the section which satisfies the target reliability level is expressed as:

$$\beta_i(\hat{\mathbf{s}}) = \beta_{T_i} \quad (4.1)$$

where β_{T_i} is the target reliability in the i -direction and $\hat{\mathbf{s}}$ is coefficient vector about geometric parameter. Generally one can find an optimum section by solving the equation (4.1), and in this research uses Newton-Raphson method for solving non-linear equations. Procedure of Newton-Raphson method is represented in (4.2).

$$\begin{aligned}
\hat{\mathbf{s}}_{k+1} &= \hat{\mathbf{s}}_k + \Delta\hat{\mathbf{s}} \\
\beta_i(\hat{\mathbf{s}}_{k+1}) &= \beta_i(\hat{\mathbf{s}}_k + \Delta\hat{\mathbf{s}}) \approx \beta_i(\hat{\mathbf{s}}_k) + \frac{\partial\beta_i}{\partial\hat{\mathbf{s}}} \Delta\hat{\mathbf{s}} \approx \beta_{T_i} \\
\Delta\hat{\mathbf{s}} &= \left(\frac{\partial\beta_i}{\partial\hat{\mathbf{s}}}\right)^{-1} (\beta_{T_i} - \beta_i(\hat{\mathbf{s}}_k))
\end{aligned} \tag{4.2}$$

The sensitivity of reliability index with respect to geometric coefficient is obtained by FDM (finite difference method). To calculate the finite difference, another reliability index is calculated for geometric parameter which is increased by infinitesimal values.

$$\frac{\partial\beta_i}{\partial\hat{s}_j} \approx \frac{\Delta\beta_i}{\Delta\hat{s}_j} = \frac{\beta_{i,2} - \beta_{i,1}}{\hat{s}_{j,2} - \hat{s}_{j,1}} \tag{4.3}$$

where \hat{s}_j is j -th element of geometric parameters, $\beta_{i,1}$ is a reliability index for original geometric parameter $\hat{s}_{j,1}$ and $\beta_{i,2}$ is a reliability index for $\hat{s}_{j,2}$ which is increased by $\Delta\hat{s}_j$ from $\hat{s}_{j,1}$. As the geometric parameters increased, the changes of load effects also should be considered.

$$\mathbf{F} = \mathbf{C}\mathbf{q} = \begin{bmatrix} P_{DC} & P_{DW} & P_{WS} \\ M_{DC} & M_{DW} & M_{WS} \end{bmatrix} \begin{pmatrix} DC \\ DW \\ WS \end{pmatrix} \tag{4.4}$$

Among the components of the load effect matrix, dead load caused by self-weight of the RC column and wind load affecting column are influenced by changes of the gross area of concrete. Dead load caused by pylon self-weight is related to the size of the gross sectional area of the column and wind load is proportional to linear scale of the cross section.

4.2 Determination of RC pylon Sections for Uniaxial Target reliability

The optimum RC pylon cross section for uniaxial target reliability satisfies the target reliability in critical direction. Among transverse and longitudinal directions, the one which has smaller reliability index for initial cross section is decided for critical direction.

The equation for determination of the section which satisfies the target reliability in the critical direction is shown in (4.5)

$$\begin{aligned} \beta(\hat{\mathbf{s}}) &= \beta_T \\ \hat{\mathbf{s}} &= (A_g, A_s)^T \end{aligned} \tag{4.5}$$

Here, β_T is the target reliability index in the critical direction and geometric coefficient vector $\hat{\mathbf{s}}$ consists of the gross area of concrete, A_g and the gross area of reinforcement, A_s .

The optimum cross section is determined by Newton-Raphson method (4.2). The linear scale of concrete cross section is changed with the same scale in both of transverse and longitudinal directions

Since there are one equation and two unknown quantities, another equation is needed to solve the problem. In this study, two different equations are considered. One is the reinforcement ratio equation and the other is regularization function.

For the first method, when the additional reinforcement ratio equation is given, it reduces one unknown quantity because the area of reinforcement can be expressed by reinforcement ratio and the area of concrete.

$$\beta(A_g, A_s) = \beta(A_g, \rho A_g) = \beta(A_g) = \beta_T \quad (4.6)$$

Second method is to solve the equation (4.5) by using regularization function. In this method, problem is changed to minimization problem whose object function is equation (4.5) with regularization function. Regularization function can be set for any constraint condition. The condition for the constraints of concrete and reinforcement area is adopted for the regularization function in this study.

$$\text{Min}_{A_g, A_{st}} \Pi = [\beta(A_g, A_{st}) - \beta_T]^2 + \lambda[(1-\alpha)\left(\frac{A_{st}}{A_{st}^0} - r_s\right)^2 + \alpha\left(\frac{A_g}{A_g^0} - r_g\right)^2] \quad (4.7)$$

where λ and α denote regularization coefficient and weighting factor, respectively. Regularization coefficient controls the importance of the regularization term: the solution satisfies the object function well as λ becomes smaller and vice versa. Therefore it is important to choose proper λ value to get reasonable solution which satisfies object function well and also has smaller condition number of system matrix.

Equation (4.7) can be transformed in incremental form and expressed in matrix form (4.8):

$$\begin{aligned} & \begin{bmatrix} \frac{\partial \beta}{\partial A_{st}} \frac{\partial \beta}{\partial A_{st}} + \frac{\lambda(1-\alpha)}{(A_{st}^0)^2} & \frac{\partial \beta}{\partial A_{st}} \frac{\partial \beta}{\partial A_g} \\ \frac{\partial \beta}{\partial A_g} \frac{\partial \beta}{\partial A_{st}} & \frac{\partial \beta}{\partial A_g} \frac{\partial \beta}{\partial A_g} + \frac{\lambda\alpha}{(A_g^0)^2} \end{bmatrix} \begin{pmatrix} \Delta A_{st} \\ \Delta A_g \end{pmatrix} \\ & = \begin{pmatrix} \frac{\partial \beta}{\partial A_{st}} (\beta_T - \beta(\mathbf{S}_k)) + \frac{\lambda(1-\alpha)}{A_{st}^0} \left(r_s - \frac{(A_{st})_k}{A_{st}^0}\right) \\ \frac{\partial \beta}{\partial A_g} (\beta_T - \beta(\mathbf{S}_k)) + \frac{\lambda\alpha}{A_g^0} \left(r_g - \frac{(A_g)_k}{A_g^0}\right) \end{pmatrix} \end{aligned} \quad (4.8)$$

4.3 Determination of RC pylon Sections for Biaxial Target reliability

The optimum RC pylon section for biaxial target reliability satisfies the target reliability in both transverse and longitudinal directions. The equations and the unknown quantities are followed:

$$\begin{aligned}\beta_y(\hat{\mathbf{s}}) &= \beta_{T_y}, \beta_x(\hat{\mathbf{s}}) = \beta_{T_x} \\ \hat{\mathbf{s}} &= (s_x, s_y, A_{st})^T\end{aligned}\tag{4.9}$$

where β_y and β_x are target reliability index in transverse and longitudinal directions, respectively. The symbol s_y and s_x denote linear scale of the cross section in transverse and longitudinal directions, respectively, and the changed cross section area is $A_g = s_x s_y A_g^0$ where the original cross sectional area is denoted A_g^0 .

The cross section that satisfies biaxial target reliability also can be determined by Newton-Raphson method. A difference from uniaxial case is that the linear scales of cross section in each direction are not the same but independent of each other. Since there are two equations and three unknown quantities, another equation is needed. Thus, reinforcement ratio equation or regularization function could be added to solve the problem.

If the additional reinforcement ratio is given, the number of geometric parameter reduced in two and the optimum cross section can be determined by solving the following minimization problem (4.11)

$$A_s = \rho A_g = \rho s_x s_y A_g^0 \quad (4.10)$$

$$\text{Min}_{s_x, s_y} \Pi = (\beta_y(s_x, s_y) - \beta_{T_y})^2 + (\beta_x(s_x, s_y) - \beta_{T_x})^2 \quad (4.11)$$

When equation (4.11) is transformed in incremental form, the matrix equation is expressed in (4.12).

$$\begin{aligned} & \begin{bmatrix} \left(\frac{\partial \beta_1}{\partial s_x}\right)^2 + \left(\frac{\partial \beta_2}{\partial s_x}\right)^2 & \frac{\partial \beta_1}{\partial s_x} \frac{\partial \beta_1}{\partial s_y} + \frac{\partial \beta_2}{\partial s_x} \frac{\partial \beta_2}{\partial s_y} \\ \frac{\partial \beta_1}{\partial s_x} \frac{\partial \beta_1}{\partial s_y} + \frac{\partial \beta_2}{\partial s_x} \frac{\partial \beta_2}{\partial s_y} & \left(\frac{\partial \beta_1}{\partial s_y}\right)^2 + \left(\frac{\partial \beta_2}{\partial s_y}\right)^2 \end{bmatrix} \begin{pmatrix} \Delta s_x \\ \Delta s_y \end{pmatrix} \\ & = \begin{pmatrix} \frac{\partial \beta_1}{\partial s_x} (\beta_{T_1} - \beta_1) + \frac{\partial \beta_2}{\partial s_x} (\beta_{T_2} - \beta_2) \\ \frac{\partial \beta_1}{\partial s_y} (\beta_{T_1} - \beta_1) + \frac{\partial \beta_2}{\partial s_y} (\beta_{T_2} - \beta_2) \end{pmatrix} \end{aligned} \quad (4.12)$$

When the additional regularization condition is given, the problem turns into a minimization problem (4.13). The object function makes reliability indices to be equal to target reliability indices and the regularization term constrain the area of concrete and reinforcement.

$$\text{Min}_{s_x, s_y, A_{st}} \Pi = (\beta_y - \beta_{T_y})^2 + (\beta_x - \beta_{T_x})^2 + \lambda[(1-\alpha)\left(\frac{A_{st}}{A_g^0} - r_s\right)^2 + \alpha\left(\frac{A_g}{A_g^0} - r_g\right)^2] \quad (4.13)$$

The equation above is expressed (4.14) in incremental form.

$$\begin{aligned} & \left[\begin{array}{cc} \left(\frac{\partial\beta_y}{\partial s_x}\right)^2 + \left(\frac{\partial\beta_x}{\partial s_x}\right)^2 + \lambda\alpha \frac{1}{(A_g^0)^2} \left(\frac{\partial A_g}{\partial s_x}\right)^2 & \frac{\partial\beta_y}{\partial s_x} \frac{\partial\beta_y}{\partial s_y} + \frac{\partial\beta_x}{\partial s_x} \frac{\partial\beta_x}{\partial s_y} + \lambda\alpha \frac{1}{(A_g^0)^2} \frac{\partial A_g}{\partial s_x} \frac{\partial A_g}{\partial s_y} & \frac{\partial\beta_y}{\partial s_x} \frac{\partial\beta_y}{\partial A_{st}} + \frac{\partial\beta_x}{\partial s_x} \frac{\partial\beta_x}{\partial A_{st}} \\ & \left(\frac{\partial\beta_y}{\partial s_y}\right)^2 + \left(\frac{\partial\beta_x}{\partial s_y}\right)^2 + \lambda\alpha \frac{1}{(A_g^0)^2} \left(\frac{\partial A_g}{\partial s_y}\right)^2 & \frac{\partial\beta_y}{\partial s_y} \frac{\partial\beta_y}{\partial A_{st}} + \frac{\partial\beta_x}{\partial s_y} \frac{\partial\beta_x}{\partial A_{st}} \\ \text{sym.} & & \left(\frac{\partial\beta_y}{\partial A_{st}}\right)^2 + \left(\frac{\partial\beta_x}{\partial A_{st}}\right)^2 + \lambda(1-\alpha) \frac{1}{(A_{st}^0)^2} \end{array} \right] \\ & \times \begin{pmatrix} \Delta s_x \\ \Delta s_y \\ \Delta A_{st} \end{pmatrix} = \begin{pmatrix} \frac{\partial\beta_y}{\partial s_x} (\beta_{T_y} - \beta_y) + \frac{\partial\beta_x}{\partial s_x} (\beta_{T_x} - \beta_x) - \lambda\alpha \frac{1}{A_g^0} \left(\frac{A_g}{A_g^0} - r_g\right) \frac{\partial A_g}{\partial s_x} \\ \frac{\partial\beta_y}{\partial s_y} (\beta_{T_y} - \beta_y) + \frac{\partial\beta_x}{\partial s_y} (\beta_{T_x} - \beta_x) - \lambda\alpha \frac{1}{A_g^0} \left(\frac{A_g}{A_g^0} - r_g\right) \frac{\partial A_g}{\partial s_y} \\ \frac{\partial\beta_y}{\partial A_{st}} (\beta_{T_y} - \beta_y) + \frac{\partial\beta_x}{\partial A_{st}} (\beta_{T_x} - \beta_x) - \lambda(1-\alpha) \frac{1}{A_{st}^0} \left(\frac{A_{st}}{A_{st}^0} - r_s\right) \end{pmatrix} \end{aligned} \quad (4.14)$$

5. Application and Verification

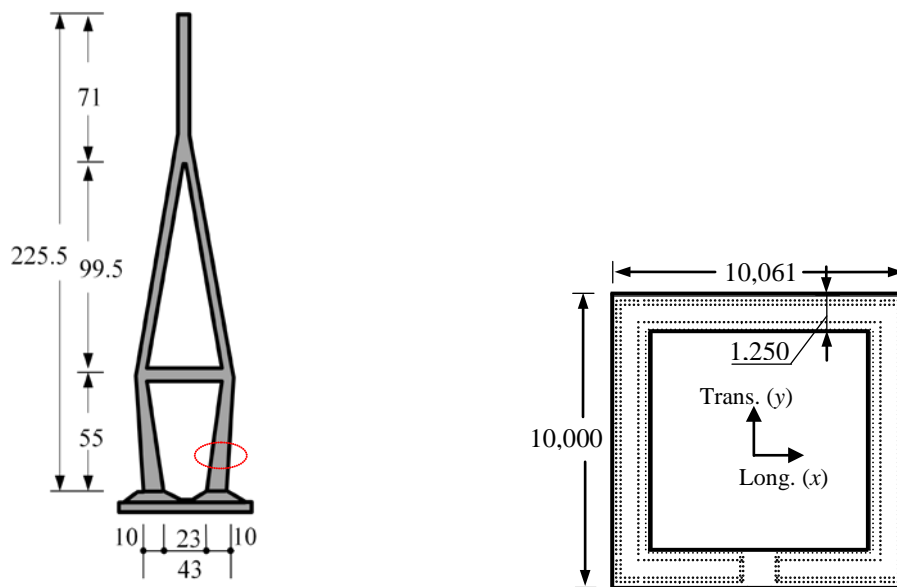
The validity of reliability analysis with the assumption of UDRC column is demonstrated for two examples, and the optimum sections for uniaxial and biaxial target reliability index are determined by the method introduced in paragraph 4.

The example bridges are Incheon Bridge and Ulsan Bridge which are selected as examples of cable-stayed bridge and suspension bridge, respectively. The cross sections are selected from lower part of the pylons. As the wind load combination usually dominates in the case of pylon of cable bridges, the target reliability index is set for 3.1 as proposed in KHBDC.

When one uses reinforcement ratio equation for finding the optimum sections, the reinforcement ratio was set in the range of 1% to 4% as the concrete design code proposed. If the regularization functions are added to solve the problem, weighting factor α is changed in the range of 0 to 1. After finding the optimum sections by two different methods, the results were compared in the reinforcement ratio range of 1% to 4%. And the reliability indices were checked after placing the general rebar in the sections for one case of reinforcement ratio for each example.

5.1 Incheon Bridge

Incheon Bridge is a cable-stayed bridge located in Incheon and it connects Yeongjong Island and the mainland of Incheon. The total length is 21.38 km and the height of pylon is 225.5 m. The pylon and the cross section of lower part is shown in Fig. 5.1.



(a) Front view of pylon (unit: m)

(b) Cross section of pylon (unit: mm)

Fig. 5.1 Pylon and cross section of Incheon Bridge

The statistical properties of pylon of Incheon Bridge are shown in Table 5.1.

Table 5.1
Statistical properties of random variables for cross section of Incheon Bridge pylon

Random variable	Nominal value	Bias factor	COV	Distribution type	
Material properties	f_{ck}	45 MPa	1.158	0.095	Lognormal
	f_y	400 MPa	1.150	0.080	Lognormal
	E_s	200 GPa	1.000	0.060	Lognormal
Geometric properties	e_s	0.0 mm	1.000	-	Normal
	A_{st}	1.46 m ² ($\rho = 0.0403$)	1.000	0.015	Normal
	A_g	36.14 m ²	1.010	0.000	Normal
Load parameters	DC_p	1.00	1.050	0.100	Normal
	DC_g	1.00	1.030	0.080	Normal
	DW	1.00	1.000	0.250	Normal
	WS	1.00	1.123	0.288	Extreme-type I

The gross area of concrete in original cross section is $A_g = 36.14 \text{ m}^2$, and the gross area of reinforcement is $A_s = 1.46 \text{ m}^2$ with around 4% of reinforcement ratio. The symbol e_s in the Table 5.1 is position error of the rebar. Normal distribution with zero mean is assumed for position error, and the radius of each rebar is taken as the standard deviation. Therefore the location of k -th rebar is denoted $y_{s,k} = \hat{y}_{s,k} + e_{s,k}$ where $\hat{y}_{s,k}$ denotes the exact position of the rebar.

Table 5.2 shows the load effect of Incheon Bridge. The wind load is used for design life of 100 years and can be separated in two values, the wind load on the pylon,

WS_p and the wind load on the other components of the bridge except the pylon, WS_{etc} .

Table 5.2 Load effect of cross section of Incheon Bridge pylon

Load direction	Total nominal load effects	Load effect matrix				Deterministic values	
		DC_p	DC_g	DW	WS		
Tans.	P_q (MN)	175.18	115.87	82.05	30.42	-52.59	-0.57
	M_q (MN·m)	644.42	-117.77	-25.95	-24.19	712.91	99.41
Long.	P_q (MN)	226.34	115.87	82.05	30.42	-0.72	-1.27
	M_q (MN·m)	364.27	0.00	105.05	-99.77	334.68	24.32

Table 5.3 Composition of wind load of Incheon Bridge

Load direction	Total WS	WS_p	WS_{etc}
Transverse	-52.59	-20.91	-31.68
	712.91	352.71	360.20
Longitudinal	-0.72	-0.67	-0.05
	334.68	287.05	47.63

5.1.1 Result of reliability analysis

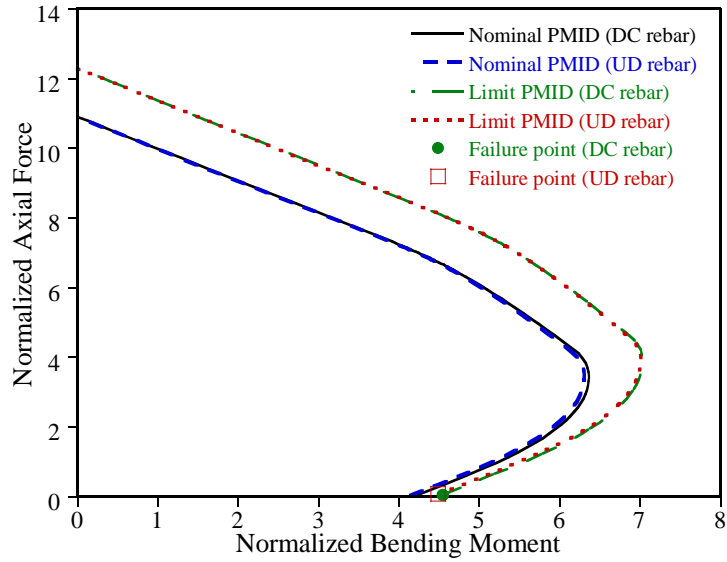


Fig. 5.2 Nominal and limit PMIDs and MPFPs of Incheon Bridge in transverse direction

Table 5.4
Reliability index and normalized MPFP of Incheon Bridge in transverse direction

Rebar type	Reliability index	Normalized MPFP									
		Material properties			Geometric properties			Load parameters			
		f_{ck}	f_y	E_s	$(e_s)_{avg.}$	$A_s/A_{st.}$	A_g	DC_p	DC_g	DW	WS
DC	4.65	1.15	1.07	1.00	0.00	1.00	1.01	1.02	1.02	0.96	4.21
UD	4.61	1.15	1.07	1.00	-	1.00	1.01	1.02	1.02	0.96	4.16

The results of reliability analysis for general reinforcement (DC rebar) and uniformly distributed reinforcement (UD rebar) are shown in Fig. 5.2. Two of PMIDs

and the MPFPs coincide and the reliability index and normalized MPFPs are shown in the Table 5.4.

Reliability analysis could not be done in longitudinal direction because the reliability index was too big and it overs the significant digit of calculation. Therefore critical direction for uniaxial target reliability was decided as transverse direction.

5.1.2 Determination of pylon section for uniaxial target reliability

Fig. 5.3 and Fig. 5.4 show the results of optimum sections for uniaxial target reliability by using reinforcement ratio equation and regularization function, respectively. The optimum section is obtained by adjusting the original cross section by s_{A_g} scale for concrete and s_{A_s} scale for reinforcement.

The comparison between the results of two methods is shown in Fig.5.5. The results of two methods are in agreement with each other. That is, when the reinforcement ratio is decided, the optimum section for uniaxial target reliability is determined for a unique solution.

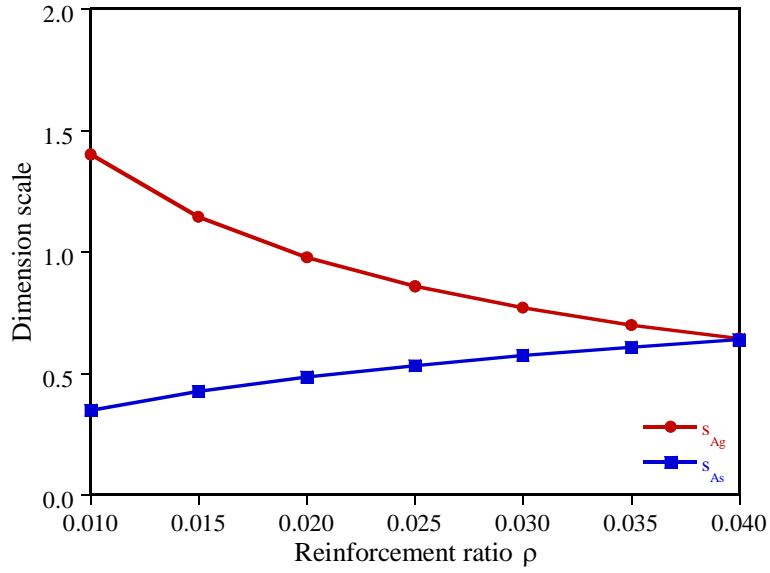


Fig. 5.3 Dimension scale of geometric parameters for uniaxial target reliability under given reinforcement ratio

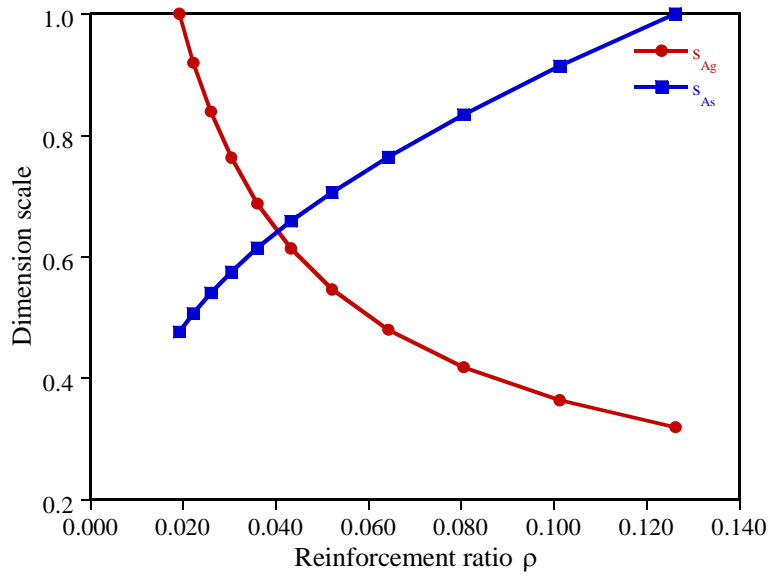


Fig. 5.4 Dimension scale of geometric parameters for uniaxial target reliability under given regularization function

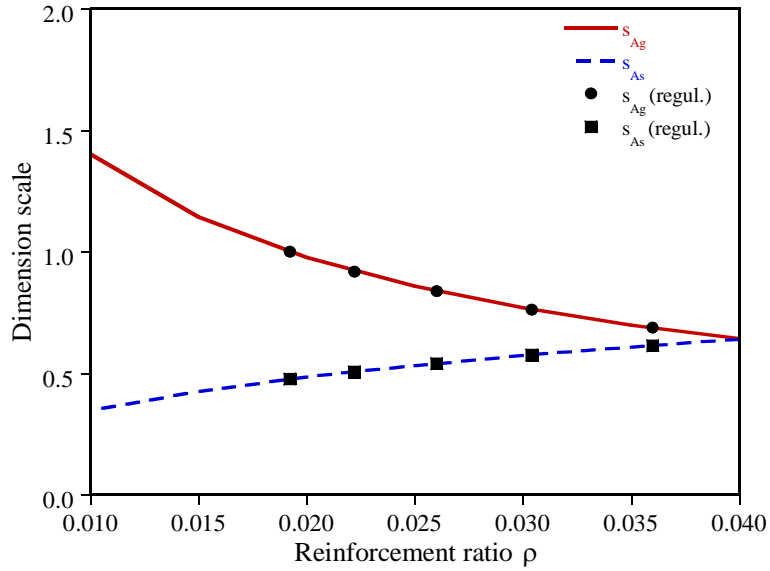


Fig. 5.5 Comparison of results for condition of reinforcement ratio and regularization function

To verify the reliability indices for general reinforcement cases, reliability analysis are conducted for the section that has discretely located rebar correspond to 4% of reinforcement ratio. The location of rebar is determined on the basis of original design section. The adjusted cross section is shown in Fig. 5.6 and limit PMIDs and MPFPs are shown in Fig. 5.7. The reliability indices and normalized MPFPs are summarized in the Table 5.5. The results satisfy the target reliability.

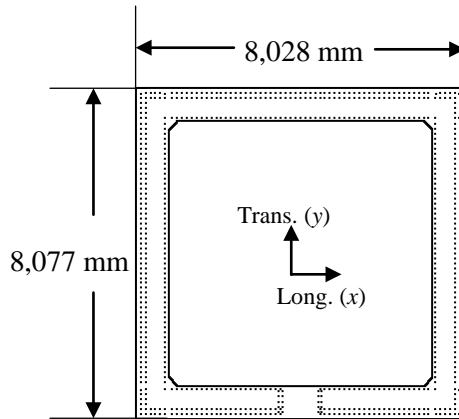


Fig. 5.6 Optimum section for uniaxial target reliability of 4% reinforcement ratio with general rebar

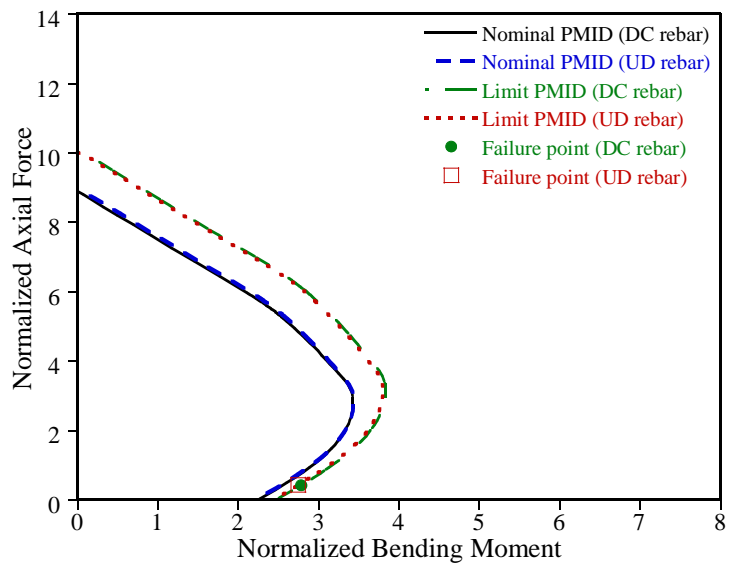


Fig. 5.7 Nominal and limit PMIDs and MPFPs for 4% reinforcement cross section

Table 5.5 Reliability index and normalized MPFP of 4% reinforcement cross section in transverse direction

Rebar type	Reliability index	Normalized MPFP									
		Material properties			Geometric properties			Load parameters			
		f_{ck}	f_y	E_s	$(e_s)_{avg.}$	$A_s/A_{st.}$	A_{gt}	DC_p	DC_g	DW	WS
DC	3.14	1.15	1.10	1.00	0.00	1.00	1.01	1.03	1.02	0.97	2.72
UD	3.10	1.15	1.10	1.00	-	1.00	1.01	1.03	1.02	0.97	2.68

5.1.3 Determination of pylon section for biaxial target reliability

Fig. 5.8 and Fig. 5.9 are the results of optimum sections for biaxial target reliability by using reinforcement ratio equation and regularization function, respectively. Here, transverse and longitudinal directions are denoted x and y .

For determination of the optimum section, the length of the original section is changed by s_x scale in longitudinal direction and s_y scale in transverse direction. Then the changed section is denoted $A_g = s_x s_y A_g^0 = s_{A_g} A_g^0$, where A_g^0 is the area of original section and s_{A_g} is the scale of concrete area. Since the reliability index of original section is bigger in longitudinal direction, longitudinal linear scale s_x adjusted smaller than transverse linear scale s_y in Fig 5.8 and Fig. 5.9.

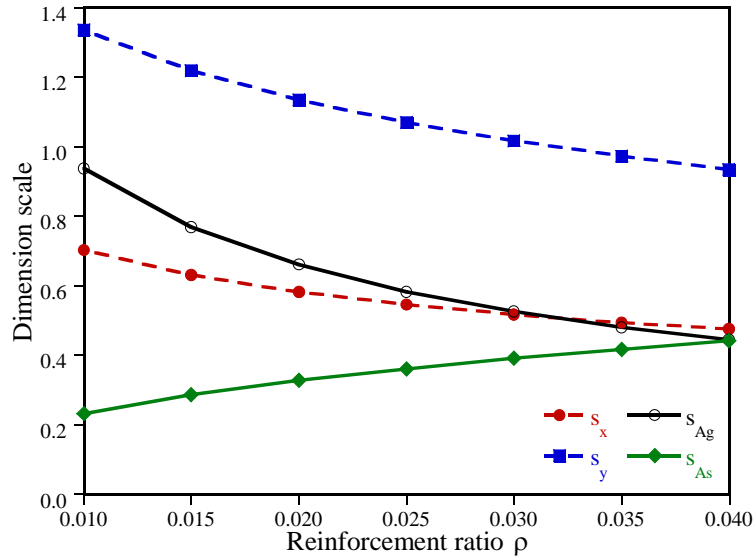


Fig. 5.8 Dimension scale of geometric parameters for biaxial target reliability Under given reinforcement ratio

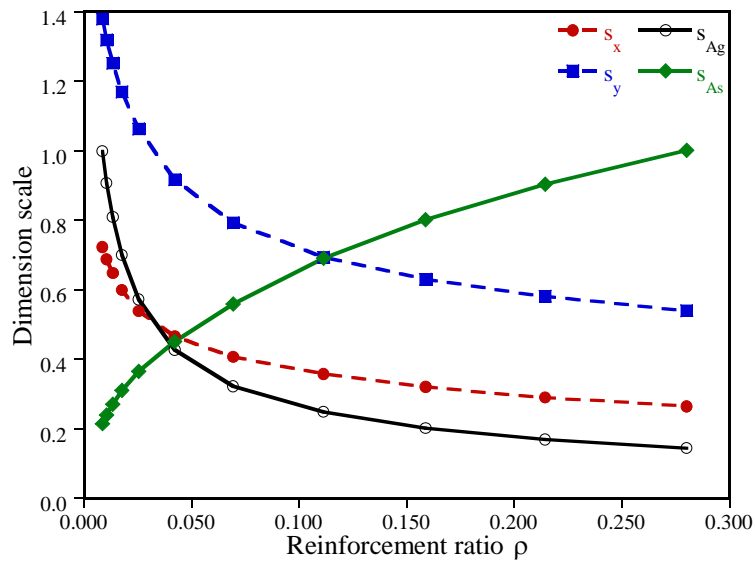


Fig. 5.9 Dimension scale of geometric parameters for biaxial target reliability under given regularization function

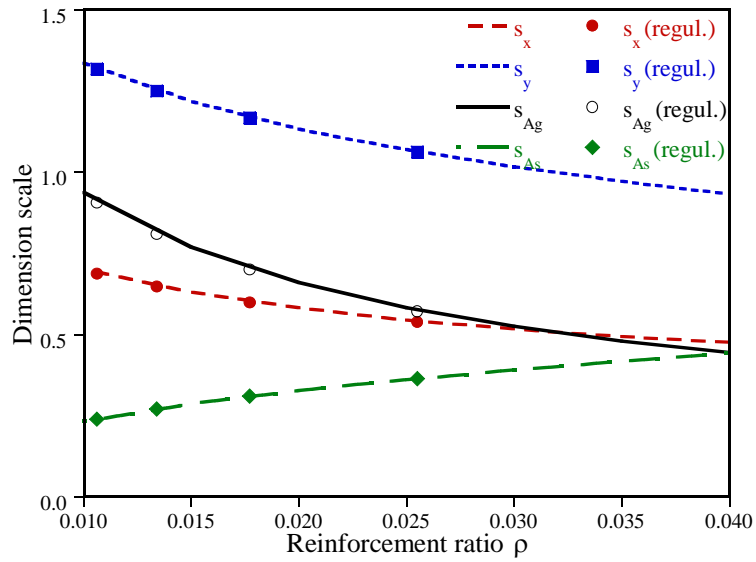


Fig. 5.10 Comparison of results for condition of reinforcement ratio and regularization function

Fig. 5.10 shows the comparison between the results of two methods. The lines and the dotted lines show the result of reinforcement ratio condition and the markers show the result of the regularization condition. The optimum section for biaxial target reliability is determined for a unique solution, when the reinforcement ratio is decided.

To verify the reliability indices for general reinforcement cases, discrete rebar is positioned for the 4% reinforcement ratio section. Fig. 5.11 shows the adjusted section and Fig.5.12 and Fig. 5.13 are limit PMIDs and MPFPs in transverse and longitudinal direction, respectively. The reliability indices and normalized MPFPs are shown in the Table 5.6 and Table 5.7. The both of sections with discrete rebar and uniformly distributed reinforcement satisfy the target reliability in both directions.

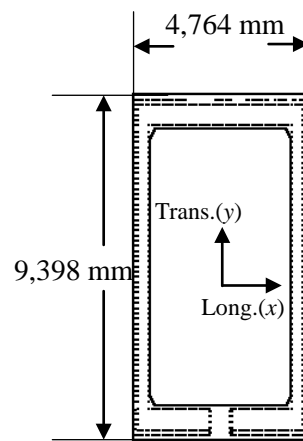


Fig. 5.11 Optimum section for biaxial target reliability of 4% reinforcement ratio with general rebar

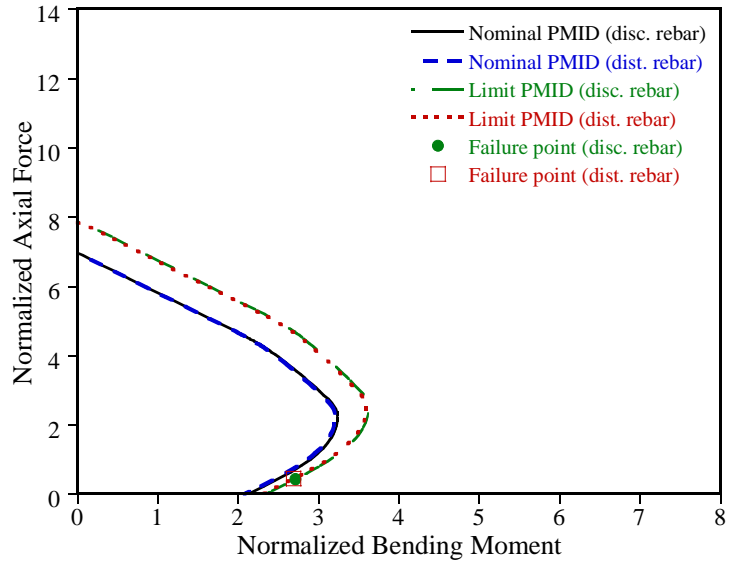


Fig. 5.12 Nominal and limit PMIDs and MPFPs for 4% reinforcement cross section in transverse direction

Table 5.6 Reliability index and normalized MPFP of 4% reinforcement cross section in transverse direction

Rebar type	Reliability index	Normalized MPFP									
		Material properties			Geometric properties				Load parameters		
		f_{ck}	f_y	E_s	$(e_s)_{avg.}$	$A_s/A_{st.}$	A_{gt}	DC_p	DC_g	DW	WS
DC	3.13	1.15	1.10	1.00	0.00	1.00	1.01	1.04	1.02	0.95	2.72
UD	3.10	1.15	1.10	1.00	-	1.00	1.01	1.04	1.02	0.95	2.68

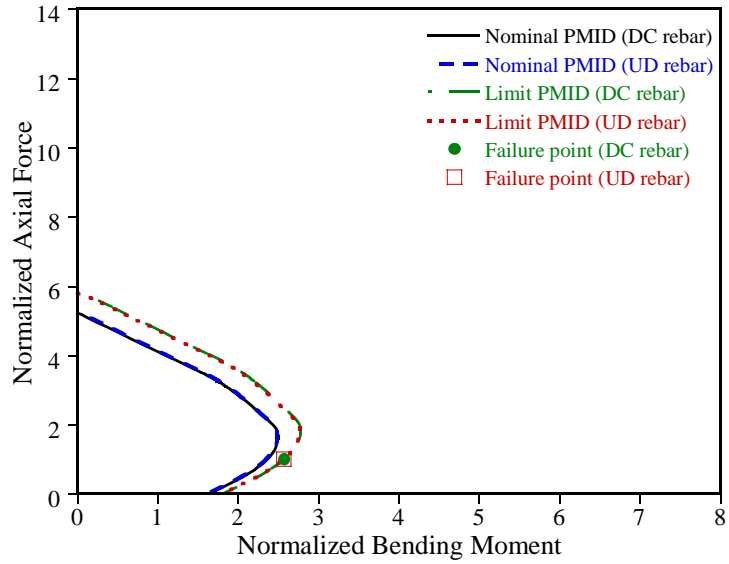


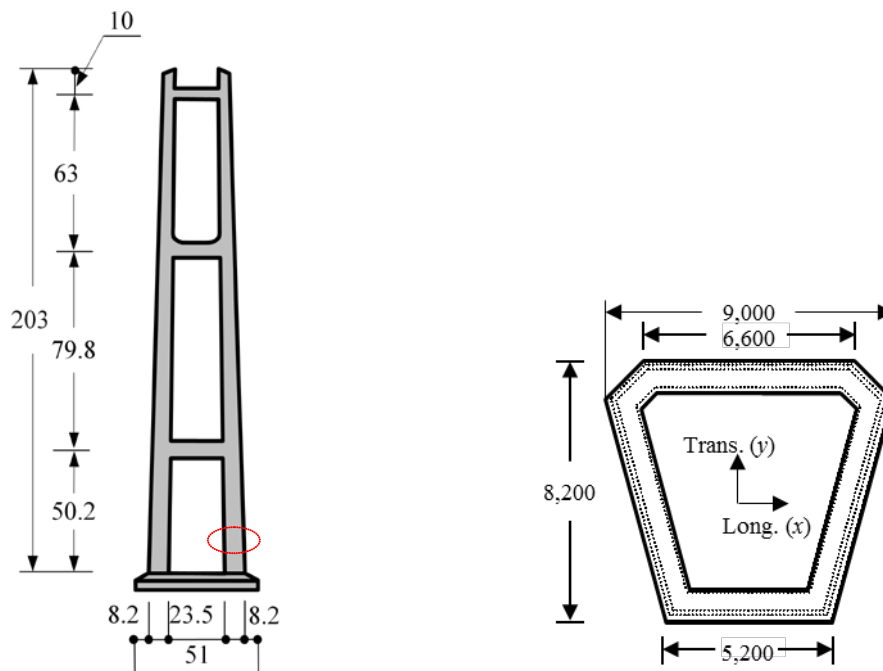
Fig. 5.13 Nominal and limit PMIDs and MPFPs for 4% reinforcement cross section in longitudinal direction

Table 5.7 Reliability index and normalized MPFP of 4% reinforcement cross section in longitudinal direction

Rebar type	Reliability index	Normalized MPFP									
		Material properties			Geometric properties			Load parameters			
		f_{ck}	f_y	E_s	$(e_s)_{avg.}$	$A_s/A_{st.}$	A_{gt}	DC_p	DC_g	DW	WS
DC	3.13	3.11	1.13	1.11	1.00	0.00	1.00	1.01	1.04	1.03	0.90
UD	3.10	3.09	1.13	1.11	1.00	-	1.00	1.01	1.04	1.03	0.91

5.2 Ulsan Bridge

Ulsan Bridge is a suspension bridge whose total length is 1.8 km and the height of the pylon is 203 m. The pylon and the cross section of lower part are shown in Fig. 5.14. The statistical properties of pylon of Ulsan Bridge are shown in Table 5.8.



(a) Front view of pylon (unit: m)

(b) Cross section of pylon (unit: mm)

Fig. 5.14 Pylon and cross section of Ulsan Bridge

Table 5.8

Statistical properties of random variables for cross section of Ulsan Bridge pylon

Random variable	Nominal value	Bias factor	COV	Distribution type	
Material properties	f_{ck}	40 MPa	1.150	0.100	Lognormal
	f_y	400 MPa	1.150	0.080	Lognormal
	E_s	200 GPa	1.000	0.060	Lognormal
Geometric properties	e_s	0.0 mm	1.000	-	Normal
	A_s	0.51 m ² ($\rho = 0.0195$)	1.000	0.015	Normal
	A_{gt}	26.18 m ²	1.010	0.000	Normal
Load parameters	DC_P	1.00	1.050	0.100	Normal
	DC_C	1.00	1.000	0.060	Normal
	DC_g	1.00	1.030	0.080	Normal
	DW	1.00	1.000	0.250	Normal
	WS	1.00	1.1466	0.3206	Extreme-type I

The gross area of concrete in original cross section is $A_g = 26.18 \text{ m}^2$, and the gross area of reinforcement is $A_s = 0.51 \text{ m}^2$ with around 2% of reinforcement ratio. Table 5.9 shows the load effect of Ulsan Bridge. The wind load is used for design life of 100 years and can be separated in wind load on the pylon and on the other components of the bridge except the pylon (Table 5.10).

Table 5.9 Load effect of cross section of Ulsan Bridge pylon

Load direction	Total nominal load effects		Load effect matrix					Deterministic values
			<i>DC_p</i>	<i>DC_c</i>	<i>DC_g</i>	<i>DW</i>	<i>WS</i>	
Tans.	P_q (MN)	166.19	104.51	30.84	65.07	15.00	-49.29	0.06
	M_q (MN·m)	319.02	-5.31	-9.13	-0.39	-0.22	251.37	82.69
Long.	P_q (MN)	213.95	104.51	30.84	65.07	15.00	-1.39	-0.07
	M_q (MN·m)	296.12	0.00	373.92	-329.68	-47.72	205.67	93.93

Table 5.10 Composition of wind load of Ulsan Bridge

Load direction	Total <i>WS</i>	<i>WS_p</i>	<i>WS_etc</i>
Transverse	-49.29	-19.72	-29.58
	251.37	123.17	128.20
Longitudinal	-1.39	-1.26	-0.14
	205.67	176.88	28.79

5.2.1 Result of reliability analysis

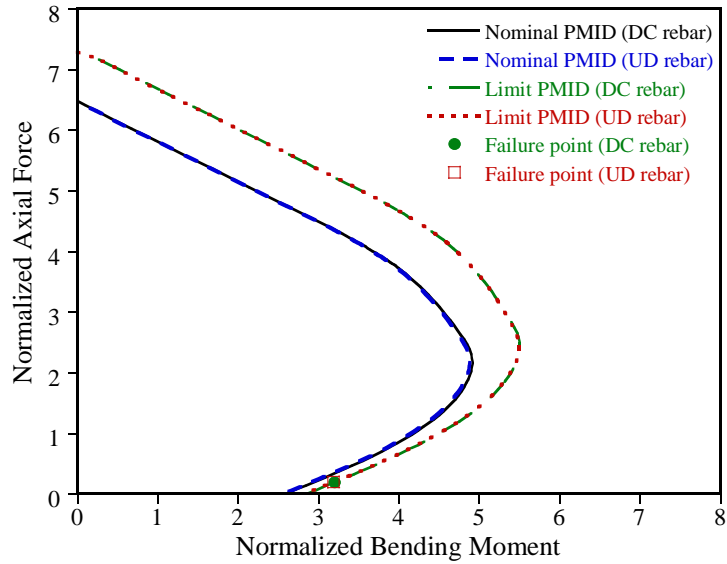


Fig. 5.15 Nominal and limit PMIDs and MPFPs of Ulsan Bridge in transverse direction

Table 5.11
Reliability index and normalized MPFP of Ulsan Bridge in transverse direction

Rebar type	Reliability index	Normalized MPFP										
		Material properties			Geometric properties				Load parameters			
		f_{ck}	f_y	E_s	$(e_s)_{av}$ g	A_s $/A_{st}$	A_{gt}	DC_p	DC_c	DC_g	DW	WS
DC	3.92	1.14	1.10	1.00	0.00	1.00	1.01	1.02	1.00	1.02	0.97	3.79
UD	3.91	1.14	1.10	1.00	-	1.00	1.01	1.02	1.00	1.02	0.97	3.78

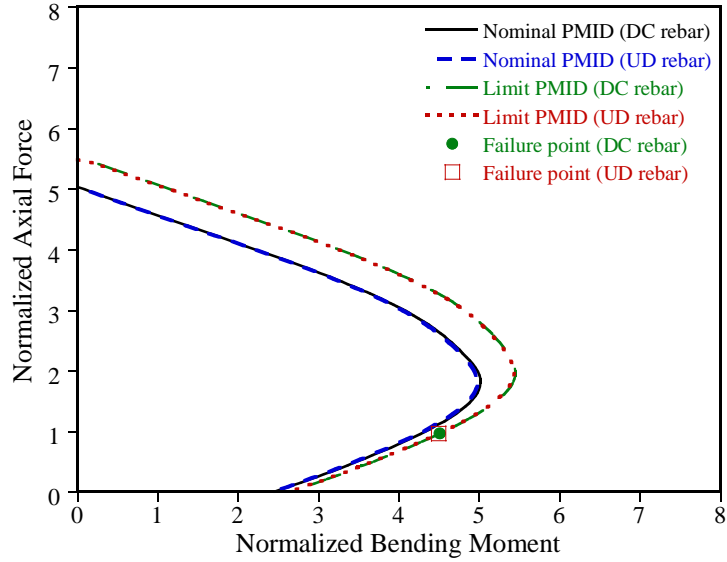


Fig. 5.16 Nominal and limit PMIDs and MPFPs of Ulsan Bridge in longitudinal direction

Table 5.12
Reliability index and normalized MPFP of Ulsan Bridge in longitudinal direction

rebar type	Reliability index	Normalized MPFP										
		Material properties			Geometric properties				Load parameters			
		f_{ck}	f_y	E_s	$(e_s)_{av}$	A_s/A_{st}	A_{gt}	DC_p	DC_c	DC_g	DW	WS
DC	5.56	1.10	1.08	1.00	0.00	1.00	1.01	1.01	1.02	0.98	0.92	5.97
UD	5.56	1.10	1.08	1.00	-	1.00	1.01	1.01	1.02	0.98	0.92	5.95

The results of reliability analysis for DC rebar and UD rebar are shown in Fig. 5.15 and Fig. 5.16 in transverse and longitudinal direction, respectively. The relative error of reliability indices between two kinds of rebar was less than 1% and the

magnitude of reliability index was bigger in longitudinal direction. Thus critical direction is decided as transverse direction.

5.2.2 Determination of pylon section for uniaxial target reliability

Fig. 5.17 and Fig. 5.18 show the results of optimum sections for uniaxial target reliability by using reinforcement ratio equation and regularization function, respectively. Two results were in agreement with each other and it is shown in Fig. 5.19.

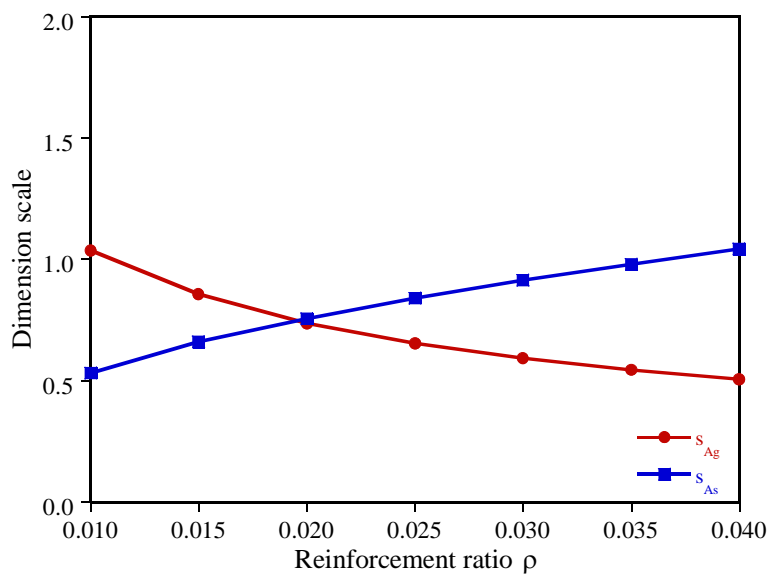


Fig. 5.17 Dimension scale of geometric parameters for uniaxial target reliability under given reinforcement ratio

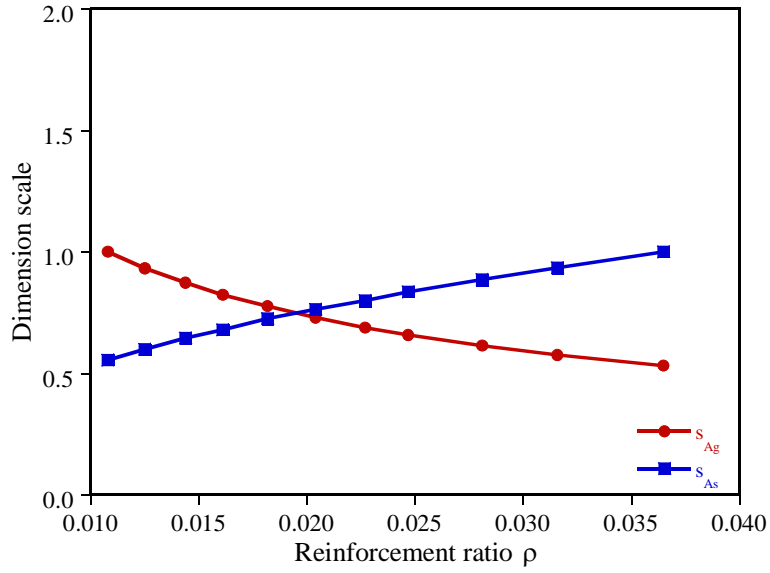


Fig. 5.18 Dimension scale of geometric parameters for uniaxial target reliability under given regularization function

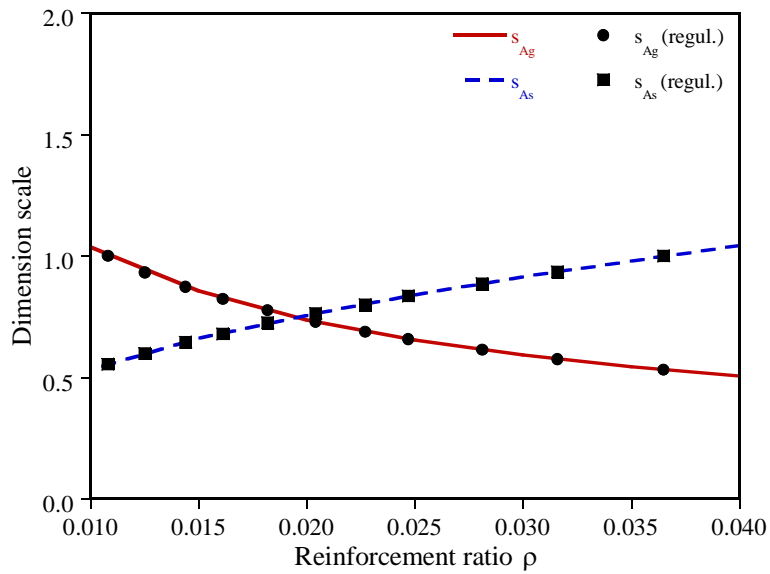


Fig. 5.19 Comparison of results for condition of reinforcement ratio and regularization function

The results of reliability analysis for the optimum section of 2% reinforcement ratio with discretely located rebar are shown in Fig. 5.21 and Table 5.13. The location of rebar is determined on the basis of original design section and the reliability index of the section satisfies the target reliability.

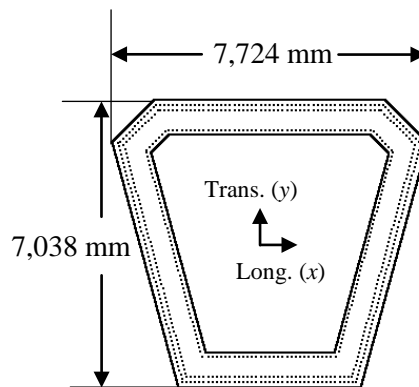


Fig. 5.20 Optimum section for uniaxial target reliability of 2% reinforcement ratio with general rebar

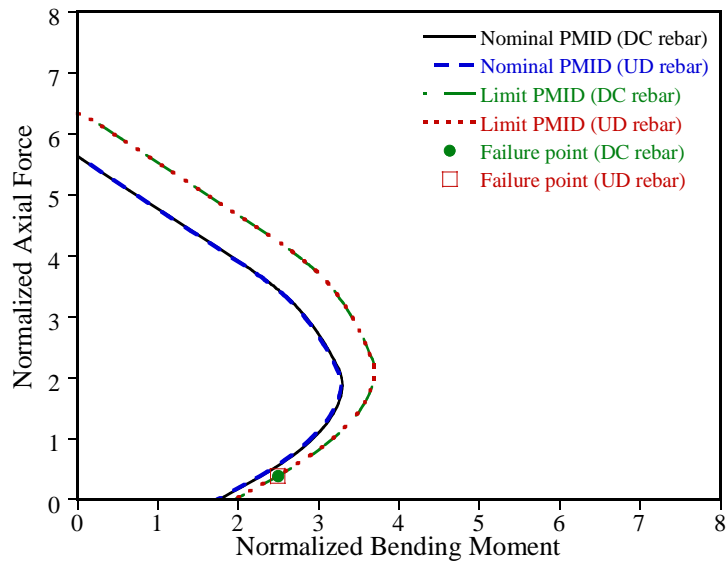


Fig. 5.21 Nominal and limit PMIDs and MPFPs for 2% reinforcement cross section

Table 5.13 Reliability index and normalized MPFP of 2% reinforcement cross section in transverse direction

Rebar type	Reliability index	Normalized MPFP										
		Material properties			Geometric properties			Load parameters				
		f_{ck}	f_y	E_s	$(e_s)_g$	A_s/A_{st}	A_{gt}	DC_p	DC_c	DC_g	DW	WS
DC	3.10	1.14	1.11	1.00	0.00	1.00	1.01	1.03	1.00	1.02	0.98	2.94
UD	3.10	1.14	1.11	1.00	-	1.00	1.01	1.03	1.00	1.02	0.98	2.93

5.2.3 Determination of pylon section for biaxial target reliability

The results of optimum sections for biaxial target reliability are shown in Fig. 5.22 and Fig. 5.23. Fig 5.22 is the result for the reinforcement ratio condition and Fig. 5.23 is the one for the regularization condition. These two results are compared in Fig 5.24 and they are in agreement with each other.

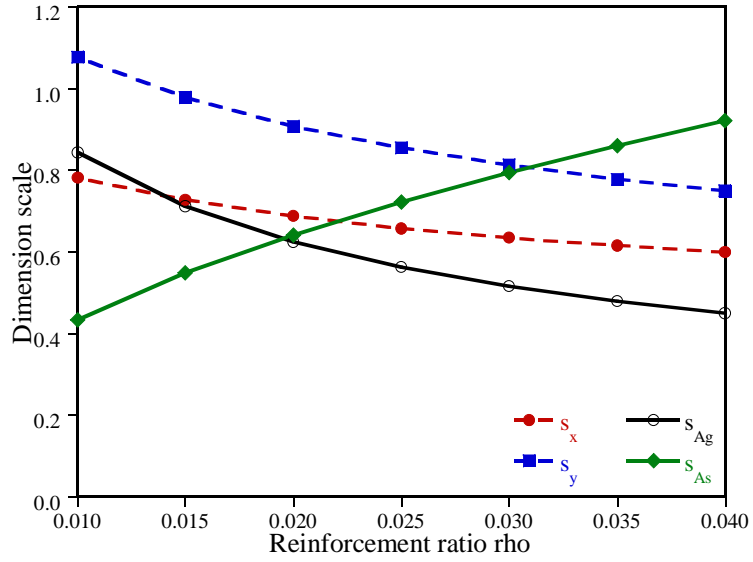


Fig. 5.22 Dimension scale of geometric parameters for biaxial target reliability under given reinforcement ratio

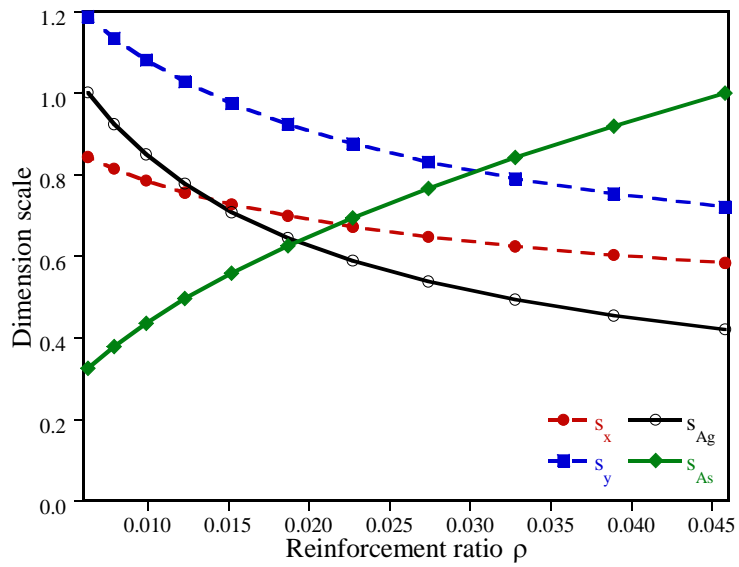


Fig. 5.23 Dimension scale of geometric parameters for biaxial target reliability under given regularization function

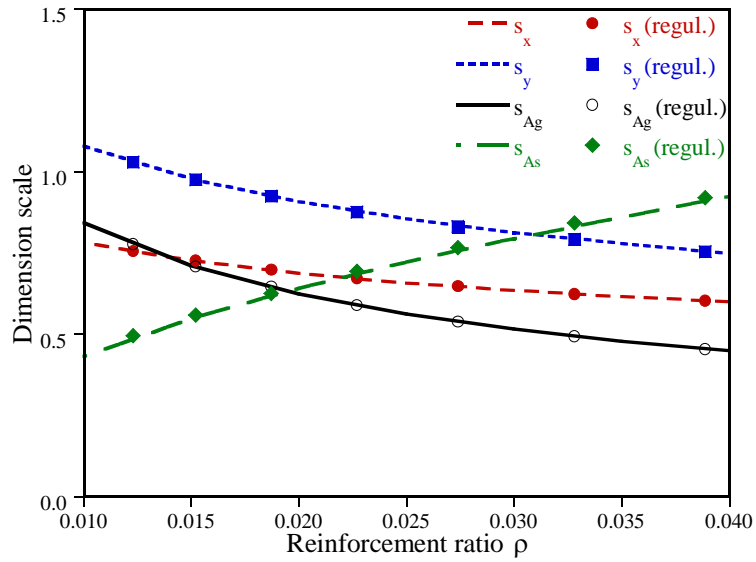


Fig. 5.24 Comparison of results for condition of reinforcement ratio and regularization function

Discrete rebar is positioned for the 2% reinforcement ratio section and reliability analysis is conducted. The results show the section satisfies the target reliability in both transverse and longitudinal directions.

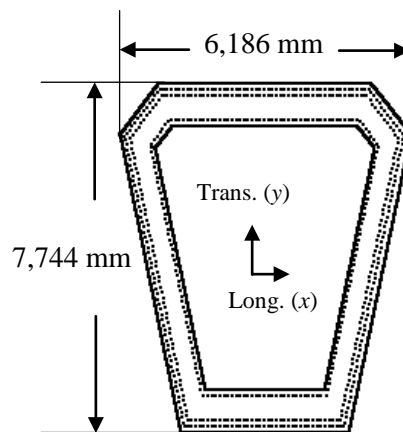


Fig. 5.25 Optimum section for biaxial target reliability of 2% reinforcement ratio with general rebar

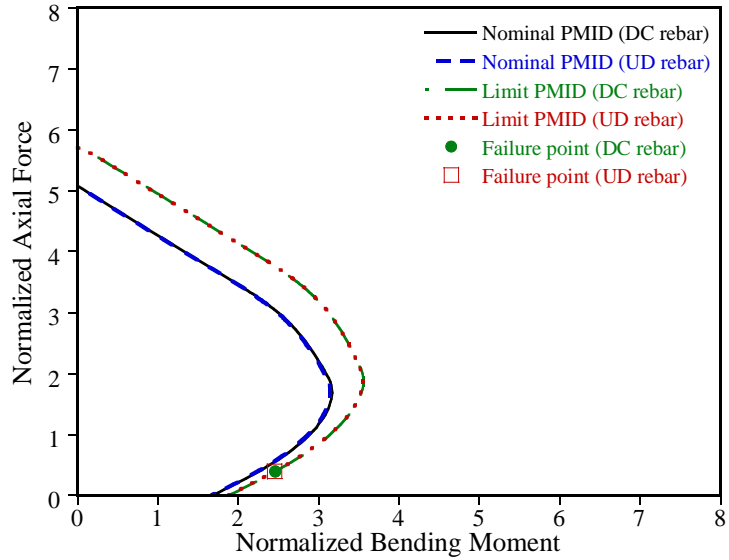


Fig. 5.26 Nominal and limit PMIDs and MPFPs for 2% reinforcement cross section in transverse direction

Table 5.14 Reliability index and normalized MPFP of 2% reinforcement cross section in transverse direction

Rebar type	Reliability index	Normalized MPFP										
		Material properties			Geometric properties				Load parameters			
		f_{ck}	f_y	E_s	$(e_s)_g$	A_s/A_{st}	A_{gt}	DC_p	DC_c	DC_g	DW	WS
DC	3.11	1.13	1.12	1.00	0.00	1.00	1.01	1.03	1.00	1.02	0.97	2.95
UD	3.10	1.14	1.12	1.00	-	1.00	1.01	1.03	1.00	1.02	0.97	2.94

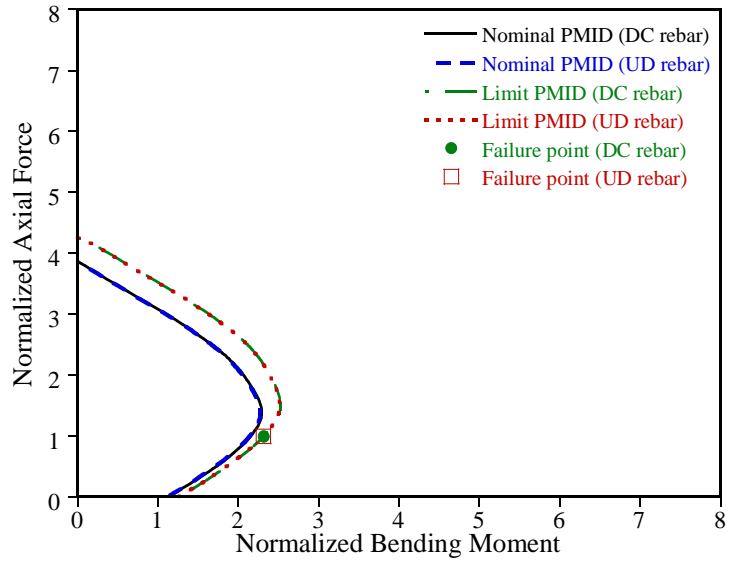


Fig. 5.27 Nominal and limit PMIDs and MPFPs for 2% reinforcement cross section in longitudinal direction

Table 5.15 Reliability index and normalized MPFP of 2% reinforcement cross section in longitudinal direction

Rebar type	Reliability index	Normalized MPFP										
		Material properties			Geometric properties				Load parameters			
		f_{ck}	f_y	E_s	$(e_s)_{av}$ g	A_s $/A_{st}$	A_{gt}	DC_p	DC_c	DC_g	DW	WS
DC	3.11	1.11	1.12	1.00	0.00	1.00	1.01	1.04	1.02	0.98	0.93	2.87
UD	3.10	1.11	1.12	1.00	-	1.00	1.01	1.04	1.02	0.98	0.93	2.86

6. Summary and Conclusion

In this study, the concept of uniformly distributed reinforcement is introduced for reinforced concrete pylon. PMID based on this uniformly distributed reinforcement was formulated and the validity of this assumption was verified by reliability analysis.

The strength of RC column section can be expressed by gross sectional area and reinforcement ratio when the UDRC is applied to the section. It is useful to introduce the UDRC assumption that the optimum section for target reliability level can be determined in general form.

The optimum section can be calculated by Newton-Raphson method with the given reinforcement ratio condition or regularization functions. When determining the optimum sections for uniaxial target reliability, the critical direction can be decided for the direction which has lower reliability level and the length of the section is changed in the same scale in both directions. Meanwhile, the optimum sections for biaxial target reliability are determined as the sections that satisfy the target reliabilities in both directions. The length of the section is changed in different scale to find the optimum section in this case.

The results for two different additional conditions coincide in each case of two examples. That is, the optimum section for uniaxial and biaxial reliability is determined for a unique solution under given reinforcement ratio.

General forms of optimum sections for target reliability are determined in two real bridge examples. It is verified that real section can be determined by placing the rebar properly based on UDRC optimum sections.

Reference

- Kim, J. H., Lee, S. H., Paik, I.Y. and Lee, H. S. (2015). " Reliability assessment of reinforced concrete column based on the P-M interaction diagram using AFOSM", *Structural Safety*, Vol.55, pp.70-79
- Haldar, A., and Mahadevan, S. (2000). Probability, Reliability and Statistical Methods in Engineering Design, John Wiley & Sons, Inc., New York, pp.181-224
- Hasofer, A. M., and Lind, N. C. (1974). "Exact and invariant second-moment code format", *J. of Eng. Mech., ASCE*, Vol. 100, No. EMI, pp.111-121
- Liu PL, Der Kiureghian A. (1991). "Optimization algorithms for structural reliability", *Structural Safety*, Vol. 9, pp.161-177
- Paik, I.Y and Hwang, E.S. (2007). *Basic Theory of Reliability and Reliability-Based Design Code*, Korea Bridge design & Engineering Research center
- Rackwitz, R., Fiessler B. (1978) "Structural reliability under combined random load sequences." *Computers & Structures*, Vol. 9, pp.489-494

Singiresu S. Rao. (2009). *Engineering Optimization: theory and practice*, New Jersey: John and Wiley & Sons.

Sørensen, J. D. (2004). *Noets in Structural Reliability Theory and Risk Analysis*, Institute of Building Technology and Structural EngineeringAalborg University

Sundararajan, C. R. (2012). *Probabilistic structural mechanics handbook: theory and industrial applications*. Springer Science & Business Media.

Văcăreanu, R., Aldea, A., & Lungu, D. (2007). *Structural Reliability and Risk Analysis*.

양영순, 서용석, 이재욱 (2002). "구조 신뢰성 공학", 서울대학교출판부

이해성, 김지현, 이호현, 이승환, 백인열 (2016). "도로교설계기준 한계상태 설계법)-케이블교량편 기술총서집." 교량설계핵심기술연구단, pp.31-39, pp.171-189.

국문 초록

이 논문에서는 신뢰도기반의 설계법에서 제시하고 있는 목표신뢰도 수준을 만족하는 철근콘크리트 주탑 단면 부재를 산정하는 방법을 제안한다. 이를 위해 철근콘크리트 주탑 단면에서 이산적으로 위치해 있는 철근을 등가의 등분포 철근으로 치환하여 PM 상관도를 작성하고 단면의 강도를 총 단면적과 철근비의 함수로 일반화한다. 등분포 철근으로 일반화된 단면에 대해 신뢰도 평가를 수행하고 목표신뢰도 지수에 일치하는 단면을 산정한다. 신뢰도 평가는 Gradient projection 방법을 적용한 HL-RF 알고리즘 (AFOSM)을 사용한다. 휨과 모멘트를 받고 있는 주탑 단면에서 교직방향과 교축방향에 대해 신뢰도 평가를 하여 신뢰도가 낮은 방향이 목표신뢰도를 확보하도록 하는 1 축 목표신뢰도 만족 단면과 양 방향 모두 목표신뢰도를 확보하도록 하는 2 축 목표신뢰도 만족 단면을 결정하는 방법을 제안한다. 각 방법에서 외부 하중에 의한 주탑 단면의 신뢰도 수준이 목표신뢰도 수준이 되도록 목적함수를 정의하고 철근비 조건 또는 정규화함수 조건을 추가하여 Newton-Raphson 방법으로 단면을 결정한다. 인천대교와 울산대교 주탑 단면을 예제로 하여 1 축과 2 축 목표신뢰도를 만족하는 단면을 산정하였고 철근비 조건과 정규화함수 조건의 결과가 일치하여 주어진

철근비에서 목표신뢰도를 만족하는 단면이 유일하게 결정됨을 확인하였다. 각 경우에서 목표신뢰도를 만족하는 등분포 철근 최적단면을 등가의 철근을 배치하였을 경우에도 목표신뢰도를 만족함을 확인하여, 등분포 철근의 최적단면을 결정한 후 실제 철근을 배근하여 최적단면을 결정하는 방법의 타당성을 검증하였다.

주요어: 주탑 단면 결정, PM 상관도, 신뢰도 해석, 목표신뢰도지수,
등분포 철근, 정규화함수

학번: 2014-20560